Mechanical and Chemical Characterization of Chitosan Hydroxyapatite Composites

A Thesis Presented

by

Hani Mubarez

to

The Graduate School

in Partial Fulfillment of the

Requirements

for the Degree of

Master of Science

in

Mechanical Engineering

Stony Brook University

May 2011

UMI Number: 1495342

UMI

Dissertation Publishing

UMI 1495342

Copyright 2011 by ProQuest LLC.

ProQuest®

Stony Brook University

The Graduate School

Hani Mubarez

We, the thesis committee for the above candidate for the

Master of Science degree, hereby recommend

acceptance of this thesis.

Dr. Chad S. Korach, Advisor, Mechanical Engineering

Dr. Oscar Lopez-Pamies, Chair, Mechanical Engineering

Dr. Gary Halada, Member, Materials Science and Engineering

This thesis is accepted by the Graduate School

Lawrence Martin
Dean of the Graduate School

ii

Abstract of the Thesis

Mechanical and Chemical Characterization of Chitosan Hydroxyapatite Composites

by

Hani Mubarez

Master of Science

in

Mechanical Engineering

Stony Brook University

2011

Hydroxyapatite is a very interesting ceramic that has been explored recently for various biomedical applications ranging from bone pastes and cements to tissue scaffolds due to its biodegradability and biocompatibility. However, its ceramic behavior makes it hard to use due to its high brittleness. It has been demonstrated in the literature that a composite of Chitosan polymer and hydroxyapatite has high mechanical strength. Chitosan is biocompatible, biodegradable, nontoxic, anti-bacterial, and is soluble in diluted acidic solutions. In this thesis, we study the effects of varying the processing parameters on the mechanical and chemical properties of the composite. The processing parameters studied include using different Hydroxyapatite/ Chitosan concentrations, the use of different acids such as malic and acetic acids, the presence of nano-hydroxyapatite, and the immersion in sodium hydroxide.

Fourier transform infrared spectroscopy (FTIR) as well as X-Ray Absorption Fine Structure (XAFS) are used to study resulting chemical variations as a result of the use of different

parameter. The results suggest that there are chemical interactions between the composite's components. The chitosan's amino group and the carboxyl group from the acid act as the glue that holds the composite together.

Also, three point bending test is used to measure the flexural strength of each composite. The three point bending test shows the weakening effect of immersion in sodium hydroxide. The flexural strength and elasticity decreased by a factor of 1/3. In addition, a three point bending test for a wet specimen that has been immersed in sodium hydroxide as well as water shows that the mechanical properties of the composite decreased by a factor of 1/100 as compared to the samples just treated with sodium hydroxide and tested dry. Other processing parameters such as changing the acid used from malic acid to acetic acid showed similar mechanical properties. This was assumed to be due to the fact that both acetic acid and malic acid have carboxyl group in common. Also, since FTIR suggests that the carboxyl is the glue that holds the composite together, it was not surprising to see similar mechanical properties when these two acids are exchanged.

Scanning electron Microscopy, SEM, was used to study the fracture surface of composite. It was shown by SEM that there was good cohesion between chitosan and hydroxyapatite. However, it was confirmed that cohesion is weakened significantly once the composite is immersed in sodium hydroxide.

Dedicated to my ever supporting parents and wife

Table of Contents

vii

List of Figures

Acknowledgments

Words cannot describe my gratitude to all those who helped me and supported me throughout my research studies. It would have been impossible to do this thesis without your help. I am greatly honored to have the opportunity to thank and acknowledge your support.

First and foremost, I would like to express my greatest gratitude to my advisor, Dr. Chad S. Korach, who patiently and consistently provided me with great guidance and assistance. Working under him provided me with precious experience and skills that I would not have otherwise acquired.

Deepest gratitude is also due to Dr. Gary Halada for his acceptance of my committee invitation and helping me greatly in understanding the FTIR and XAFS results. His help and support were crucial for my thesis.

I would like to thank Dr. Oscar Lopez-Pamies for his acceptance of my committee invitation. His insightful comments and questions are appreciated.

Also, I would like to thank Karl Nelson for his help and guidance when I started doing research and beyond.

Special thanks are also given to Jim Quinn for working with me on SEM imaging, Randy Smith at the BNL-NSLS (U2B) for his help setting up the FTIR spectroscope, Paul Northrop at the BNL-NSLS (X15B) for his help setting up the XAFS spectroscope, Prof. Sanjay Sampath for allowing the use of a vacuum pump, Dr. Brian Choi for showing me how to use it, and Chris Berghorn for help during composite processing.

Also, I thank Dr. Wei Zhao, Cunyou Lu, Changhong Cao, Richard Anger, Anupam Kundu, Tommy McCune, and Polly Lo for insightful discussions, and great support throughout the project.

I am also grateful to my friends for always pushing me harder every time, and all the fun times we had.

Last but not least, I would like to thank my family. I could not have gone this far without your love and support.

Chapter 1 **Introduction**

Hydroxyapatite/chitosan composite is a very exciting polymer composite that has been explored recently for various applications. Some applications for this composite that have been considered include using the composite as a tissue scaffold, bone paste, and reinforcing ultra-high molecular weight polyethylene for acetabular cup application. The composite can have very interesting applications due to its biodegradability and biocompatibility.

Using bio-composites such as hydroxyapatite/chitosan as bone tissue engineering substitutes solves some of the problems that other methods of treating bone defects have. For example, using autografts which uses the patient's own bone to implant in the affected area has the disadvantage in that another surgery is needed to obtain the bone. Additionally, the amount of bone a person is able to take from their own body is limited [1]. Another method is using allograft which is similar to autograft except the fact that the bone is obtained from another person's body. The major disadvantage to this method is that there is a great risk of infections and negative immune response [1].

In order to be able to use a material for tissue engineering, certain requirements must be met. The material must be biocompatible, nontoxic, and biodegradable [2]. Hydroxyapatite is an obvious candidate due to the fact that it is one of the main substances forming mineralized tissue in nature along with calcite and aragonite.

Hydroxyapatite (Figure 1.1), a calcium phosphate compound $Ca_{10}(PO4)_6(OH)_2$, is hard and brittle ceramic that has been used extensively in many biomedical applications due to its

1

osteoconductivity, biocompatibility, non-toxicity, non-inflammatory, and non-immunogenic nature [3]. Additionally, hydroxyapatite is one of the main substances forming bones. Therefore it is considered very biocompatible and has been used for treating bone defects as well as for bone substitute in the field of orthopedic surgery [4].
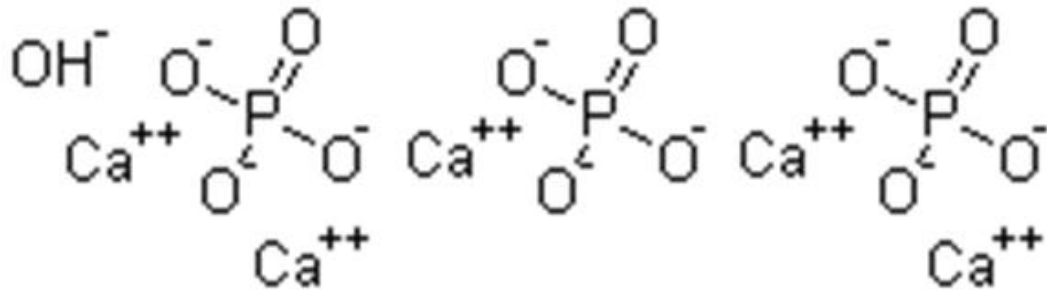
Figure 1.1: The chemical structure of hydroxyapatite

One major obstacle that renders hydroxyapatite less useful is the fact that it is very hard brittle which makes it hard to shape in specific forms needed for biomedical applications [5]. Additionally, its brittle nature causes it to be susceptible to sudden failure making it undesirable for most biomedical uses. Due to that fact, Hydroxyapatite is not usually used by itself. It is frequently incorporated in a composite with a much softer polymer to compensate for the brittleness of the hydroxyapatite [1]. Usually, this results in toughness ranging between that of the polymer and the hydroxyapatite.

One of the many organic polymers that have been considered to be used with hydroxyapatite is chitosan (Figure 1.2). Chitosan, $C_6H_{11}NO_4$, is a derivative of the naturally occurring chitin. It is a partially deacetylated derivative of chitin where there is repeat unit of $-NH_2$ group [6]. It is made of D-glucosamine (deacetylated unit) and N-acetyl-D-glucosamine (acetylated units) [7]. The amount of N-acetyl-D-glucosamine units is

2

determined by the degree of deacetylation which ranges from 70 to 95% commercially. Chitin can be found in shellfish [8]. This naturally occurring polymer readily dissolves in many acidic solutions. Additionally, it is very biocompatible, biodegradable, nontoxic, and has anti-bacterial properties [5]. Chitosan is soluble in dilute acids with PH<6 where the free amino groups in chitosan are protonated in the acid medium[h].
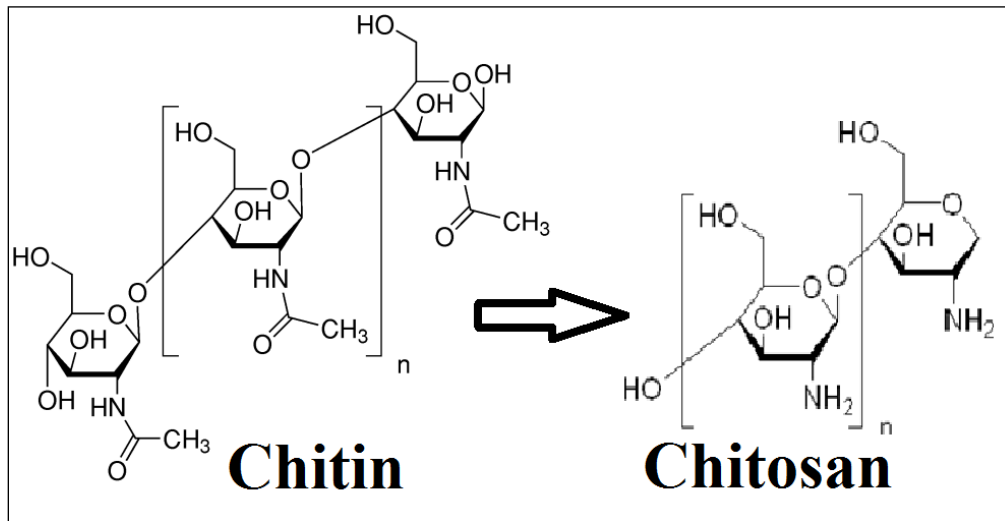
Figure 1.2: The chemical structure of chitosan (right) which is derived from chitin (left) by deacetylation (removal of acetyl group). The chitosan can have varying degree of deacetylation.

Recently, chitosan has been investigated considerably for biomedical applications. The use of chitosan micro particles as injectable carriers for cell transplantation has been explored and proved feasible [9]. There was good proliferation of goat bone marrow stromal cells as well as good adhesion between the chitosan's surface and the cells [9]. Other studies have shown that the cell proliferation and adhesion on chitosan surface can be significantly improved by enriching the chitosan's surface with fibronectin [7].

3

In other attempts, porous chitosan scaffold has been fabricated using controlled freezing and lyophilization of chitosan gels [10]. However, it was determined that the tensile strength of the porous chitosan scaffold to be ten times less than its non-porous counterpart[10]. Therefore, chitosan by itself does not have strong enough mechanical strength to allow it to serve as tissue scaffold in many areas in the body.

In the other hand, calcium phosphate cement, which has structure and composition similar to that of hydroxyapatite, has been used as bone cement that is both injectable and fast-setting by using a hardening accelerator, sodium phosphate, and a gelling agent, hydroxypropyl methylcellulose[11]. Additionally, the mechanical properties such as flexural strength, elastic modulus, and work of fracture were studied for varying processing conditions. This cement can be shaped into any desired shape due to its injectablity and fast-setting time.

Even though the chitosan scaffold and the calcium phosphate cement proved to have good potential, most attempts have been made towards making a composite containing both chitosan and hydroxyapatite due to their combined potential for biomedical applications in tissue engineering.

One such composites is a fast setting calcium phosphate cement-chitosan composite, which has been produced by mixing tetracalcium phosphate ($Ca_4(PO_4)_2O$) with dicalcium phosphate anhydrous ($CaHPO_4$) to make the calcium phosphate cement powder and mixing that with chitosan-malate solution (a solution containing malic acid and chitosan) at powder/liquid ratio of 2 while varying chitosan content by diluting the chitosan-malate solution with water [12]. The mechanical properties of the composite are studied after soaking samples of the composite in a simulated physiological solution for 20 hours prior to

4

doing the testing. It was observed that the flexural strength and elastic modulus depend on the chitosan content in the composite. The flexural strength was noted to increase from 4 MPa for pure calcium phosphate cement up to a maximum of 14 MPa for a chitosan percentage of 20% in calcium phosphate cement liquid after which it decreased. The elastic modulus followed similar trend peaking at about 4 GPA [12].

One of the composite that have been considered in literature as an improvement over Calcium phosphate cement mentioned above [11] was calcium phosphate cement-chitosan-mannitol-fiber made by incorporating chitosan, absorbable fibers and mannitol porogen to increase strength and produce macro bores for bone growth[13]. It was shown that the addition of absorbable fibers tripled the strength of the composite. However, the strength of the composite decreased as a function of immersion time in a physiological solution until it equaled that without the fibers after 42 days [13].

Another composite that incorporated both chitosan and hydroxyapatite is a composite of collagen-chitosan scaffold that was mineralized with Ca^{2+} and phosphate salts to form mineralized collagen-chitosan /hydroxyapatite scaffolds[4]. The composite was characterized by Fourier transform infrared spectroscopy (FTIR), thermal gravimetric analysis (TGA), and scanning electron microscopy (SEM). Additionally, the visco-elastic behavior of the composite was determined and compared to that of the collagen-chitosan composite. It was found that mineralized collagen-chitosan/hydroxyapatite composite had superior mechanical properties[4].

Chitosan and hydroxyapatite as part of a composite are not limited to the above but include many others. Some of these composites to list a few include chitosan polylactic acid/hydroxyapatite nano-composite[1], chitosan based polyesters and hydroxyapatite

5

composites[14], nano-hydroxyapatite/chitosan-gelatin and micro-hydroxyapatite/chitosan-gelatin composites[15], Zinc oxide containing nano-hydroxyapatite/chitosan composite[16], nano-hydroxyapatite/chitosan-Silica nano-composite[17], and chitosan-alignate porous scaffolds reinforced by nano and micro hydroxyapatite particles[18].

All these composites have something in common. They all incorporate chitosan and hydroxyapatite. Therefore, it is crucial to study these two important compounds. Many researchers have looked into chitosan/hydroxyapatite composites to understand the interaction of these two compounds and determine different methods of making a composite of chitosan and hydroxyapatite.

Chitosan/nano-hydroxyapatite composite application as a scaffold has been investigated in literature extensively. The scaffold composite has been fabricated using various methods and studied using various techniques.

A porous chitosan/nano-hydroxyapatite composite scaffold has been fabricated by mixing $Ca(NO_3)_2$ solution and $(NH_4)_2HPO_4$ solution with a 2% chitosan acetic acid solution followed by freezing at $-20^{\circ}C$, lyophilization, and finally neutralization in NaOH solution, the scaffolds were rinsed with deionized water in order to remove any remaining NaOH[3]. The composite's has been investigated physically, chemically, and biologically through SEM, porosity measurement, thermogravimetric analysis, X-ray diffraction, X-ray photoelectron spectroscopy, Fourier transformed infrared spectroscopy, and cell culturing. It has been found that the composite scaffold has better biocompatibility than its chitosan scaffold counterpart[3]. It has also been further shown that the composite has better mineralization activity allowing it to readily form carbonate hydroxyapatite on the surface

6

after immersion in simulated body fluid [19]. This layer of apatite on the surface has been shown to allow for better cell proliferation [19].

Another method of fabricating chitosan/nano-hydroxyapatite composite that has been investigated is through co-precipitation method by mixing chitosan, which has been dissolved in a 1 wt% acetic acid, with H_3PO_4 and adding the mixture slowly into Ca $(OH)_2$ suspension with vigorous stirring[20]. After the chitosan/hap composite co-precipitates, it was compressed into desired shape under 20MPa of pressure. A porous version of this composite was made by mixing NaCl particles into the co-precipitated chitosan/hydroxyapatite composite at different weight ratios to get different porosities [20]. The mechanical properties of the non-porous and porous composites were compared with and without saturated steam treatment. It was found that even though a non-porous composite has almost double the strain at fracture than that of its porous counterpart, it can be improved by steam treatment [20]. In other studies, it was found that the compressive strength of the composite varies with varying chitosan reaching a maximum value of 120 MPa for 30% chitosan and 70% nano-hydroxyapatite [21]. Additionally, it was shown that implanting the composite in the back of SD rats for 3 weeks allowed for new cell growth, but minimal inflammation even though the composite was observed to start degrading confirming the composite's biodegradability and biocompatibility [20].

Another aspect that has been studied was the effect of using medium vs. high molecular weight chitosan. It has been observed that high molecular weight chitosan/nano-hydroxyapatite composite has significantly higher compression modulus than the medium molecular weight chitosan/nano-hydroxyapatite composite [22].

7

A novel method of making nano-hydroxyapatite/chitosan scaffold composite has been done by anchoring nano-hydroxyapatite on the pore surface of chitosan scaffold [23]. This was shown to have excellent tissue regenerative properties due to its improved bioactivity as compared to the chitosan scaffold [23].

In addition to using chitosan/hydroxyapatite composite to make 3D tissue scaffold, it has been fabricated and studied in many other forms. One such form is flexible chitosan/hydroxyapatite films which can be used as a patch on bone for delivery of hydroxyapatite material [24]. The composite was made by dissolving chitosan in HCl and mixing with hydroxyapatite. The composite was characterized by FTIR, and the homogeneity of the composite was determined for different concentration of chitosan and hydroxyapatite.

Another novel form of chitosan/hydroxyapatite composite is chitosan hydrogel/hydroxyapatite membrane [25]. The effects of different processing parameter were studied using X-ray diffraction, scanning electron microscopy, Fourier transform infrared spectroscopy, Atomic force microscopy, energy-dispersive X-ray spectroscopy, and MTT assay for biocompatibility [25]. The composite was found to be useful for tissue engineering applications.

In another attempt, composite fibers of chitosan/hydroxyapatite have been made which contain chitosan in the core of the fiber and calcium phosphate mainly at the outer shell [26]. The composite's mechanical properties such as Young's modulus, breaking stress, and breaking strain were shown to depend on the concentration of chitosan.

An important study that has been done is the effect of adding citric acid to a chitosan/hydroxyapatite suspension made using co-precipitation method [5]. It was found that the addition of citric acid interacts only with the chitosan and not hydroxyapatite [5].

8

Additionally, the mechanical properties of the composite such as compressive strength and Young's modulus were enhanced for a small addition of citric acid [5].

The purpose of this study is to investigate the effect of processing parameters on the mechanical properties of the chitosan/hydroxyapatite composite. The effect of varying chitosan concentration, varying acid used in processing, inclusion of nano-hydroxyapatite particles, as well as composite treatment with sodium hydroxide. The mechanical properties that will be investigated are flexural modulus and flexural strength. Additionally, the chemical interaction between the composite components is investigated.

Chapter 2 **Chitosan Hydroxyapatite Composite Processing**

2.1. Materials

All materials used were obtained from Sigma-Aldrich. Hydroxyapatite and chitosan are chosen to be studied due to their proven biocompatibility, biodegradability, and non-toxicity. Additionally the soft polymer can serve as a matrix binding hydroxyapatite which can make the composite more stable. Acetic acid and malic acid were used in low concentrations for chitosan dissolution due to their biocompatibility and proven ability to dissolve chitosan.

Hydroxyapatite (Product# 289396) is white inorganic powder which is the main component of the composite. It has a molecular weight of 502.31 AMU, and particle size of about 10-20 μm in diameter. The elastic modulus of hydroxyapatite is about 117 GPa [27]. Nano-hydroxyapatite (product# 677418) was also used. The nano-hydroxyapatite had particle size less than 200 nm.

Medium molecular weight chitosan (Product# 448877) was also used. It has a degree of deacetylation of 75-85%. The chitosan was dissolved in DL-malic acid (Product# 240176). Malic acid has molecular weight of 134.09 AMU. The chemical structure of malic acid is shown in the figure below Figure 2.1). Another acid that was used for chitosan dissolution is acetic acid (Product# 320099). Acetic acid has molecular weight of 60.05 AMU. The chemical structure of the acetic acid is shown in the figure below (Figure 2.2).
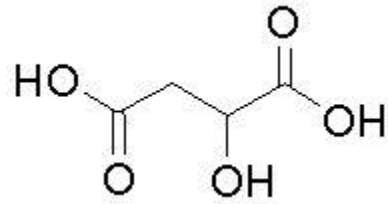
Figure 2.1: The chemical structure of malic acid
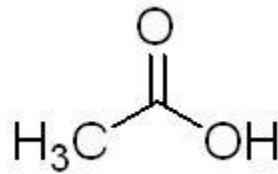
Figure 2.2: Chemical structure of acetic acid

2.2. Composite preparation and processing

The chitosan/hydroxyapatite composite was prepared using similar procedures as that used by Nelson [27]. The composite was prepared by dissolving chitosan in a 0.25M of malic acid or acetic acid. The mass fraction of chitosan in the solution is about 0.045. The chitosan solution was mixed well by stirring until the solution looked transparent and homogeneous. The resulting solution is a thick transparent gel. The chitosan solution was then left to age for 24 hours at standard lab room temperature. Then the hydroxyapatite was slowly added to the chitosan solution upon stirring. Once the hydroxyapatite was mixed well with the chitosan gel, the composite paste was vacuumed down to less than -29 inches of mercury to pull out the air bubbles from the paste. Then, it was molded on top of a flat aluminum plate followed by additional vacuum down to less than 29 inches

11

of mercury to remove any additional bubbles introduced by the molding process of the composite paste. Then, the composite paste on plate was left to dry at room temperature for at least 48 hours. Composites with varying composition were made. Table 2.1 below shows the various composites' composition.

Sample Name	Acid used	Hydroxyapatite powder/Chitosan powder ratio	Nano/Micro Hydroxyapatite Ratio
HACSMA15	Malic acid	15	0
HACSMA20	Malic acid	20	0
NanoHACSMA15	Malic acid	15	0.05
HACSAC15	Acetic Acid	15	0

Table 2.1: The different composition of the composites made. Both acids had molarity of 0.25M. The mass fraction of chitosan powder in the acid solution was 0.045.

After the composite dried, it was cut into desired dimensions. An EcoMet 3000 Polisher-Grinder was used to wet-polish the surfaces of the composite and decrease the thickness to desired level. After polishing the composite samples were left to dry at room temperature with some light weight placed on top of the samples to keep the samples flat during the initial drying time.

It was noted that the composite would easily washout in water after only 24 hours of immersion. This was improved by soaking the composite in 1M of NaOH for 24 hours. Treating the composite with NaOH was found to significantly improve the composite's anti-washout resistance.

12

Chapter 3 **Mechanical Characterization**

One of the most important aspects of this thesis is to study the effect of the processing parameters on the mechanical properties of chitosan/hydroxyapatite composite. This is important due to the fact that typical applications of interest relating to chitosan/hydroxyapatite composites is for bone repair as either a bone cement or tissue scaffold. Both applications would use the composite structurally. Therefore, mechanical strength and cohesion is very critical.

The mechanical properties of chitosan/hydroxyapatite composite were studied using three point bending test, ASTM standard D 790-00. This was used to determine the flexural strength of the composite as well as the elastic modulus for the composite.

3.1. Materials Processing and Testing

The materials were prepared as described in section 2.2 above. However, one of the samples was not immersed in NaOH. Typical samples had a length of 38.1 mm, a width of 12.7 mm, and a thickness of 1.59 mm. There was some slight variation in the samples' dimensions, but that was accounted for in the individual analysis. The samples were desiccated for at least 24 hours prior to testing with the exception of a wet sample that was immersed in water 24 hours prior to testing. Table 3.1 lists the different samples used, their composition, processing, and test conditions.

13

The testing was done using Tiratest 26005 testing frame with a load cell of 500 N. The rate of crosshead motion was about 0.7 mm/min and a span of 25.4 mm. Figure 3.1 shows the testing setup with a typical sample mounted on the fixture.
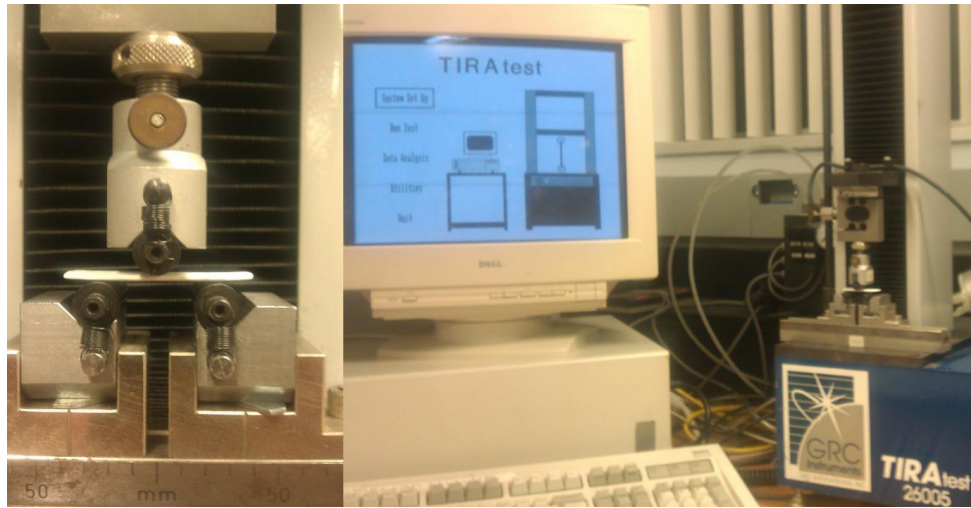
Figure 3.1: Three point bending test setup using the Tiratest 26005 machine and 500 Newton load cell.

Sample type	Hydroxyapatite powder/Chitosan powder ratio	Immersed in NaOH for 24 hours	Tested wet	Tested dry
HACSMA15	15			Yes
HACSMA15	15	Yes	Yes	
HACSMA15	15	Yes		Yes
HACSMA20	20	yes		Yes
NHACSMA15	15	Yes		Yes
HACSAC15	15	Yes		Yes

Table 3.1: Composition, processing, and test conditions of samples used for mechanical testing

14

A typical load displacement curve resulting from the three point bending test is shown in Figure 3.2 below. As can be noticed, there is a large difference between the three samples sets in terms of the maximum load at which they break as well as their slopes.
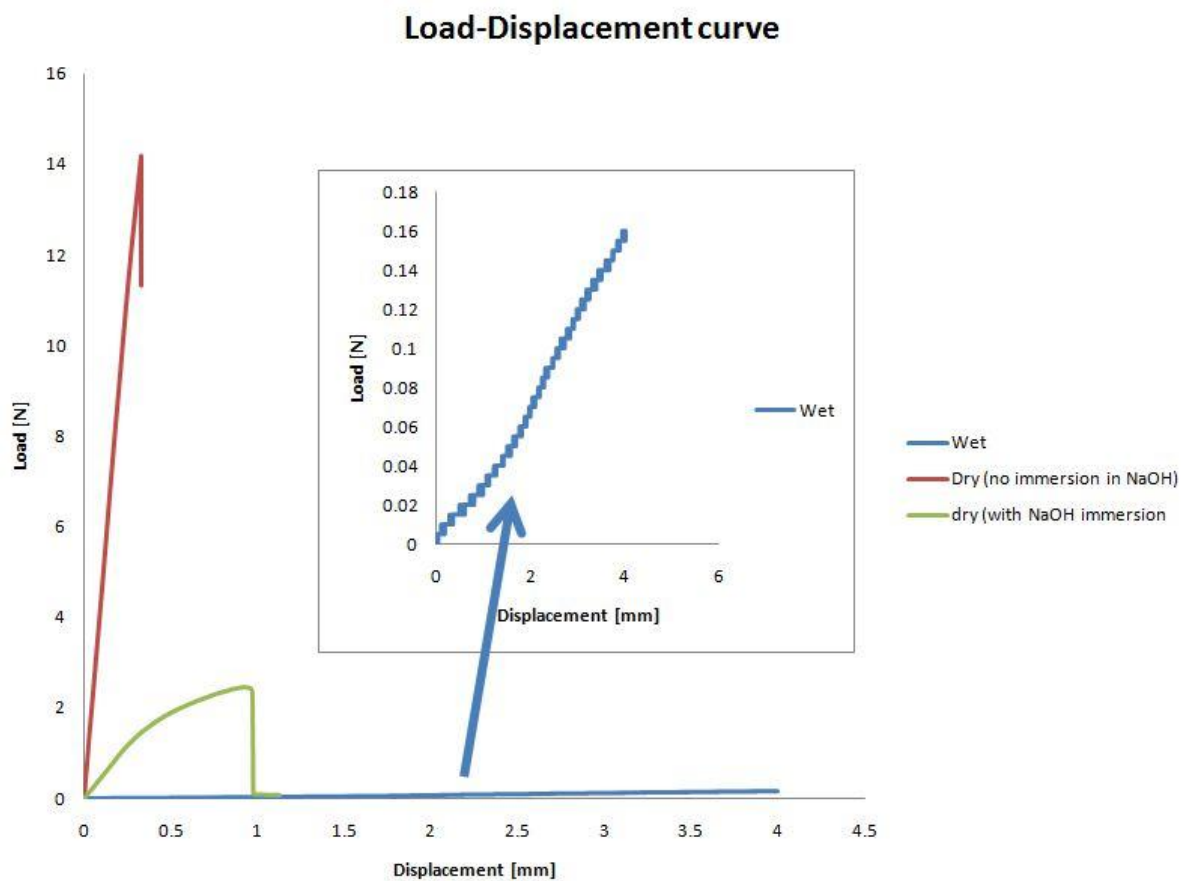
Figure 3.2: Typical load displacement curve for sample HACSMA15 for different test conditions.

The maximum force the samples were able to sustain was used to calculate the flexural strength as per eq. 3.1. Additionally, the slope of the steepest initial straight line was used to

calculate the flexural modulus as per eq. 3.2. The results are shown in Figure 3.3and Figure 3.4.

$$\sigma_{fm} = \frac{3PL}{2bd^2} \qquad \text{Eq. 3.1}$$

$$E_B = \frac{L^3m}{4bd^3} \qquad \text{Eq.3.2}$$

Where P is load, L is span, b is width, d is thickness, m is slope of the tangent to the initial straight-line portion of the load-deflection curve, E_B is modulus of elasticity at bending, and σ_{fm} is the flexural strength.

Flexural Modulus [Gpa] For Composite with HA/CS Ratio of 20

flexural strength [MPa] For Composite with HA/CS Ratio of 20

Figure 3.3: Flexural strength and modulus comparison of samples with HA/CS ratio of 20 and different processing conditions

17

Figure 3.4: Flexural strength and modulus for composites with different processing conditions
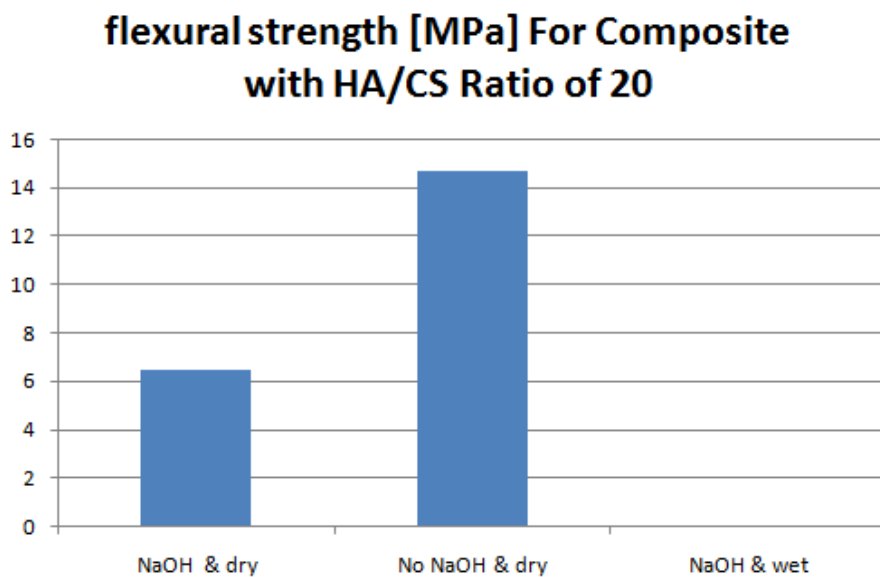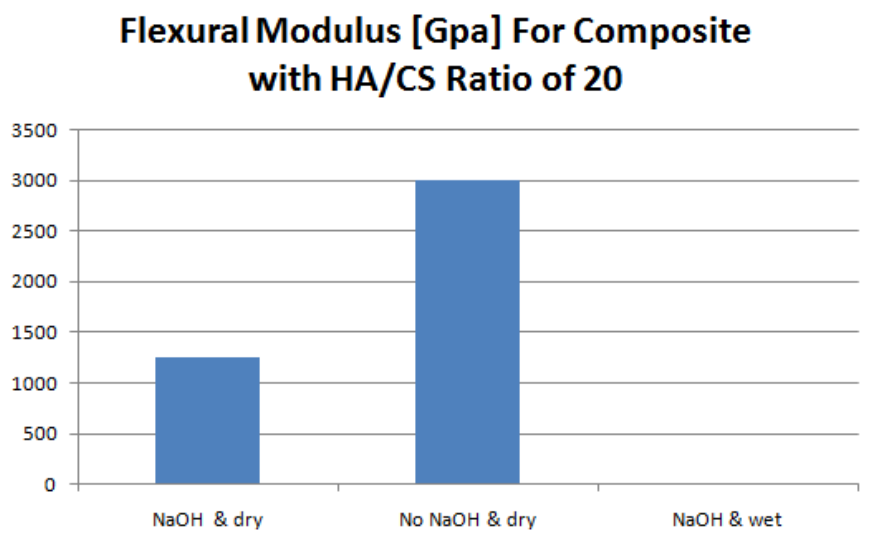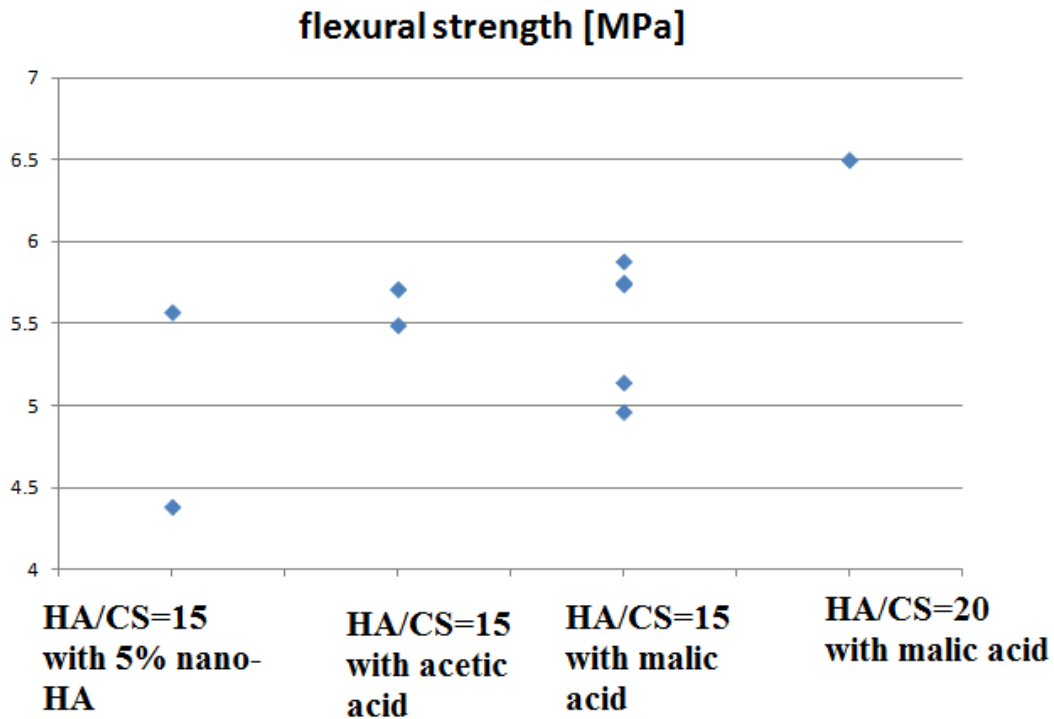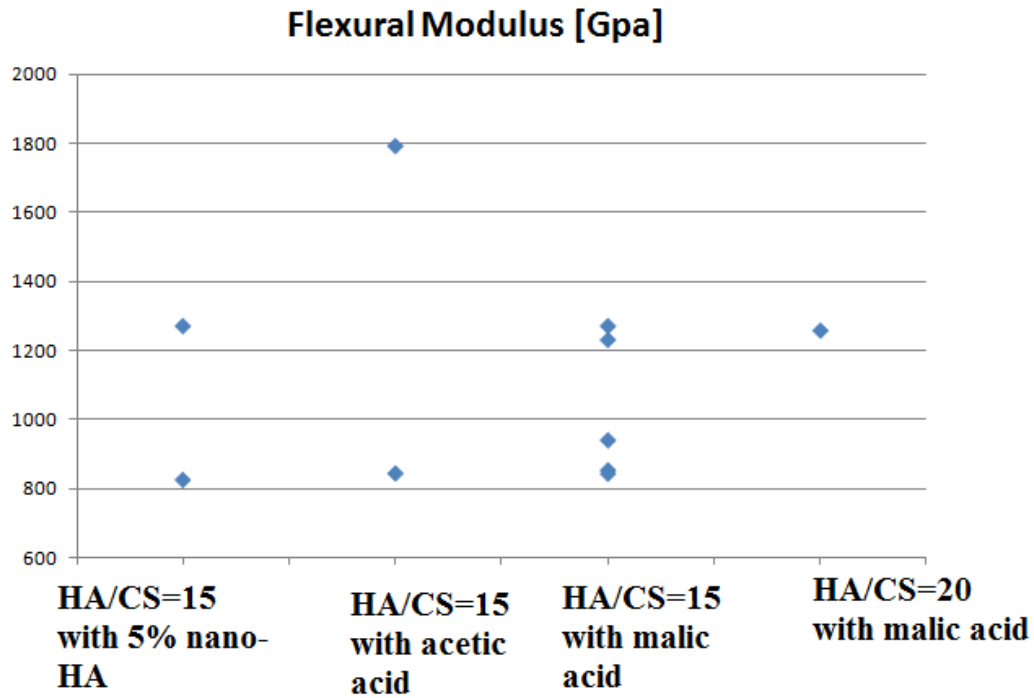
As can be noticed by comparing the different HACSMA15 samples, it is clear that the immersion of the composite in NaOH has significant detrimental effect on the mechanical strength of the composite. The flexural strength and Young's modulus of the HACSMA15 samples with no NaOH immersion is almost triple that with NaOH immersion.

Immersing the samples in NaOH was done because it proved to increase the composite's anti-washout resistance significantly. Anti-washout resistance is important due to the expected application of this composite in vivo. Sodium hydroxide can compromise the mechanical integrity of the composite by either weakening the chitosan/chitosan bonding or weakening the chitosan/hydroxyapatite bonding.

In order to investigate this, SEM imaging was done to compare the composite's fracture surface with sodium hydroxide immersion and without it. The SEM results discussed below show that the sodium hydroxide weakened the chitosan/hydroxyapatite interaction.

Additionally the composite's mechanical strength is compromised after only a day of water immersion. The Young's Modulus of the dry HACSMA15 samples is about 100 times larger than the wet sample. Also, the wet sample was very elastic; it did not even break at close to 5% strain.

This might be caused by large water absorption by the composite. Even though sodium hydroxide immersion was done to stabilize the composite if immersed in water, it seems that was not totally effective. While it did prevent the sample from breaking down and washing out after immersion in water, it was not able to completely stabilize the composite to prevent such water absorption of magnitude capable of changing the mechanical properties in such a significant way.

19

Changing the acid used to acetic acid was determined not to decrease the mechanical strength of the composite at all. However, this addition lowers the elasticity by about 0.2 GPa. The minimal change in flexural modulus due to the change in the acid used can be attributed to the fact that both acetic acids and malic acid have a carboxyl group. FTIR results discussed in Chapter 4 below confirm that the carboxyl group is the component that reacts with chitosan and hydroxyapatite.

Other parameters such as decreasing the chitosan concentration in the composite (HACSMA15, and HACSMA20) causes a small increase in both flexural strength and Young's modulus by 1 MPa and 0.3 GPa. This was expected and can be explained by the rule of mixtures for composites.

On the other hand, the addition of nano-hydroxyapatite particles along with the micro particles (HACSAC15) decreases the mechanical strength by 0.5 MPa and no change in elasticity.

SEM micrographs were done for the various chitosan/hydroxyapatite composites to investigate the morphology of the fracture surface, and fracture mechanism. Materials for SEM were prepared by mounting the fractured surface on carbon tape and coating the samples with a layer of gold to enhance conductivity to an acceptable level for SEM.
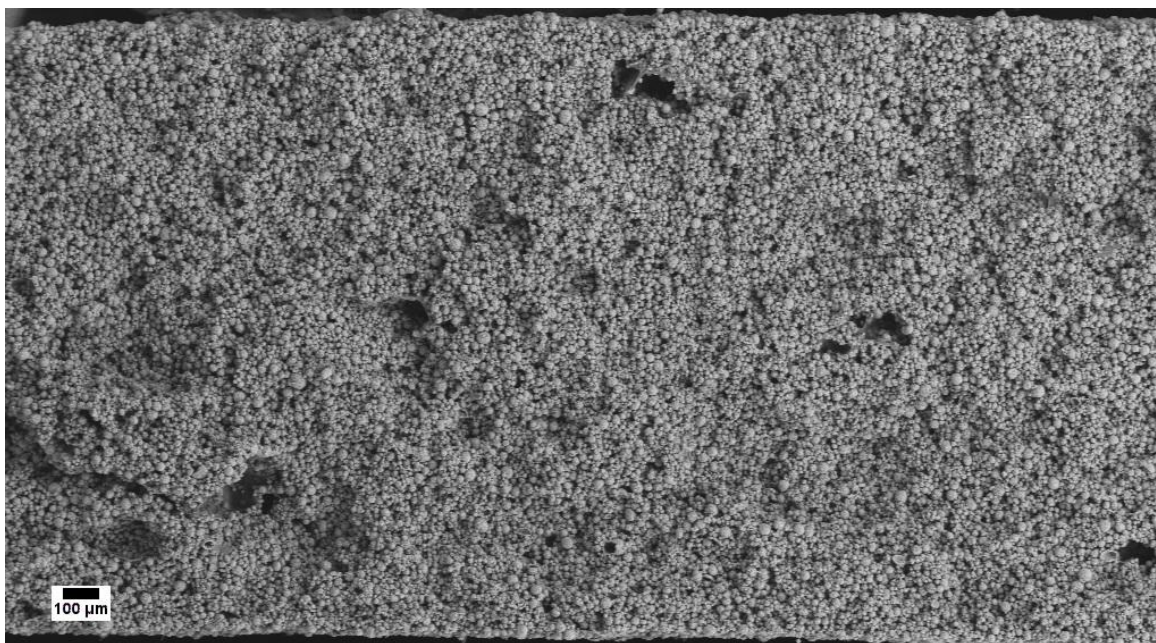
Figure 3.5: SEM of HACSMA20 fracture surface. Large pores are present throughout the composite.

As Figure 3.5 above shows, the composite has large pores throughout due to processing. The variations in the distribution of the pores can cause the mechanical properties to vary to some degree.

Figure 3.6 below shows how the chitosan matrix serves to connect the hydroxyapatite particles together. The chitosan matrix is able to hold to the hydroxyapatite particle in place

by interconnecting it to its neighboring particles. For the hydroxyapatite particle to break and not just come off the chitosan matrix means that the chitosan matrix was able to resist large stresses. There was no evidence of hydroxyapatite particle pull out from the chitosan matrix. This indicates excellent chitosan/hydroxyapatite interaction as my colleague, Karl Nelson, has shown previously [27].
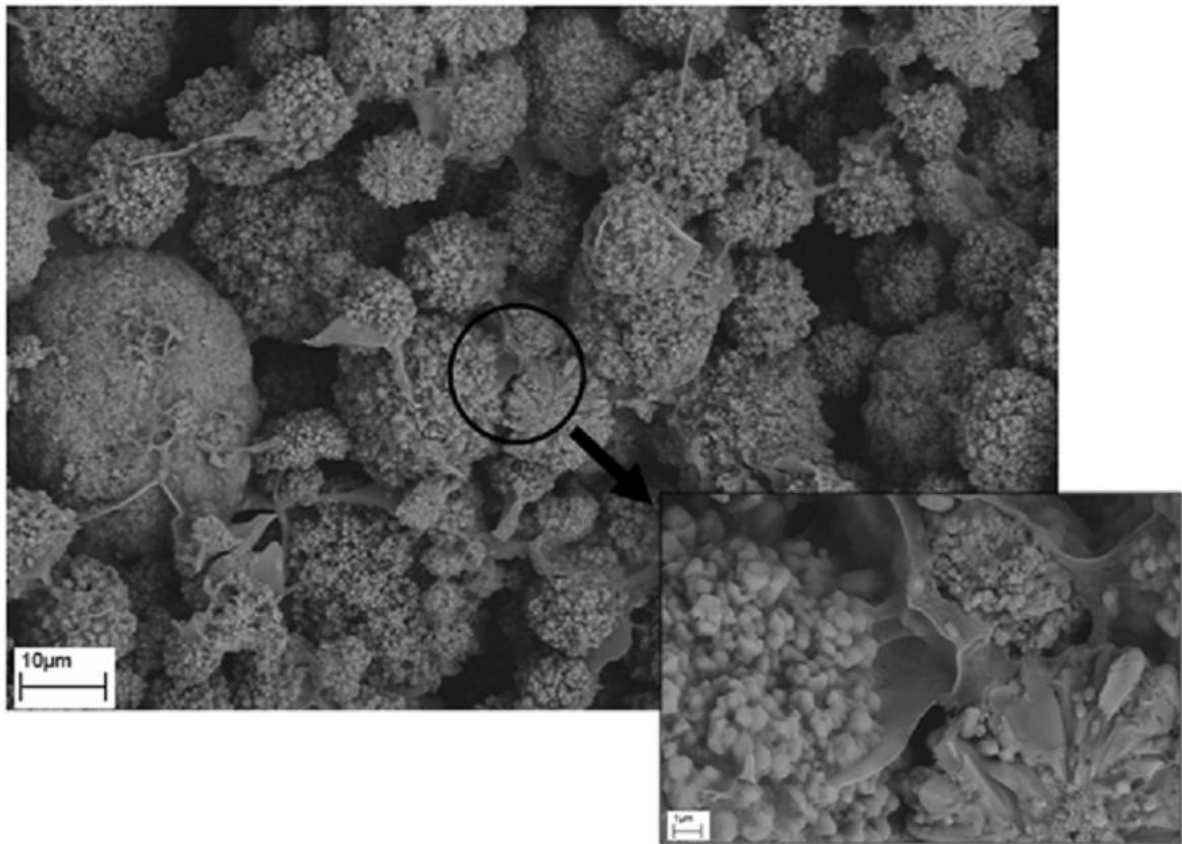
Figure 3.6: SEM of HACSMA20 fracture surface. The inset image is that of a broken hydroxyapatite particle connected by chitosan to its neighboring particles.

However, the composites that were immersed in sodium hydroxide showed exactly the opposite. There was plenty of particle pull out throughout the fracture surface (Figure 3.7- Figure 3.9). As opposed to the composite that was not soaked in sodium hydroxide

22

which showed no apparent adhesive failure, the presence of adhesive failure consistently throughout the composites soaked in sodium hydroxide indicates very poor interaction between chitosan and hydroxyapatite.
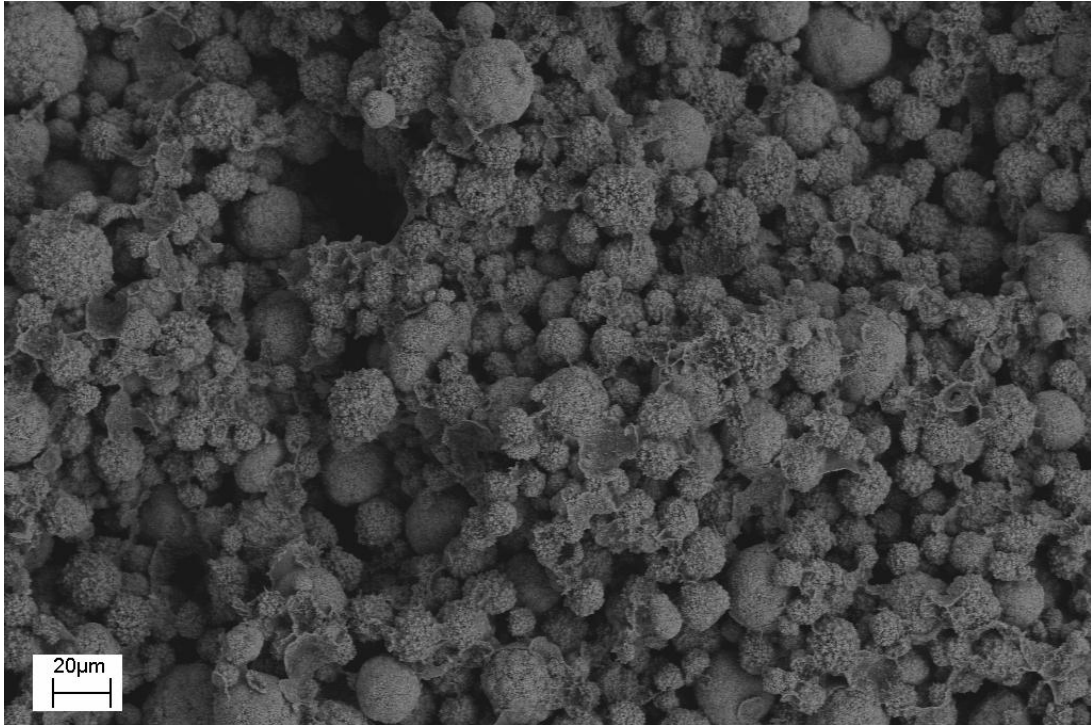
Figure 3.7: SEM of HACSMA15 fracture surface. Particle pull out locations can be seen throughout.
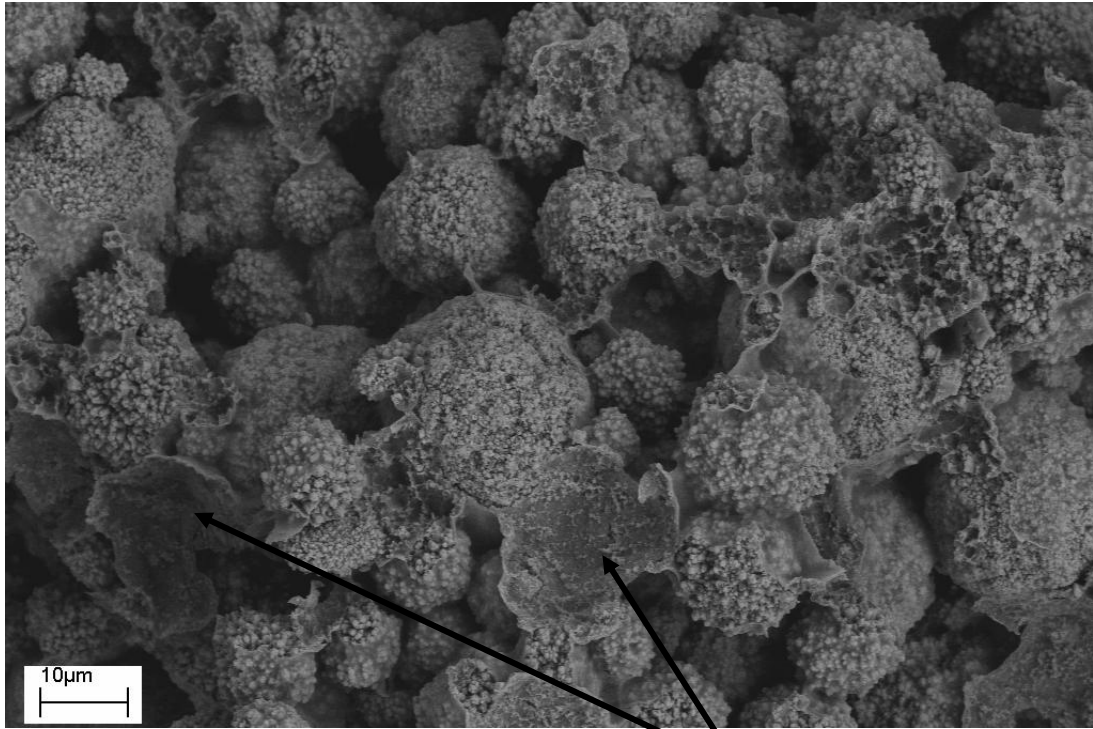
Figure 3.8: SEM of HACSMA15 fracture surface. Particle pull out locations where hydroxyapatite particles came off the chitosan matrix are indicated by the arrows.
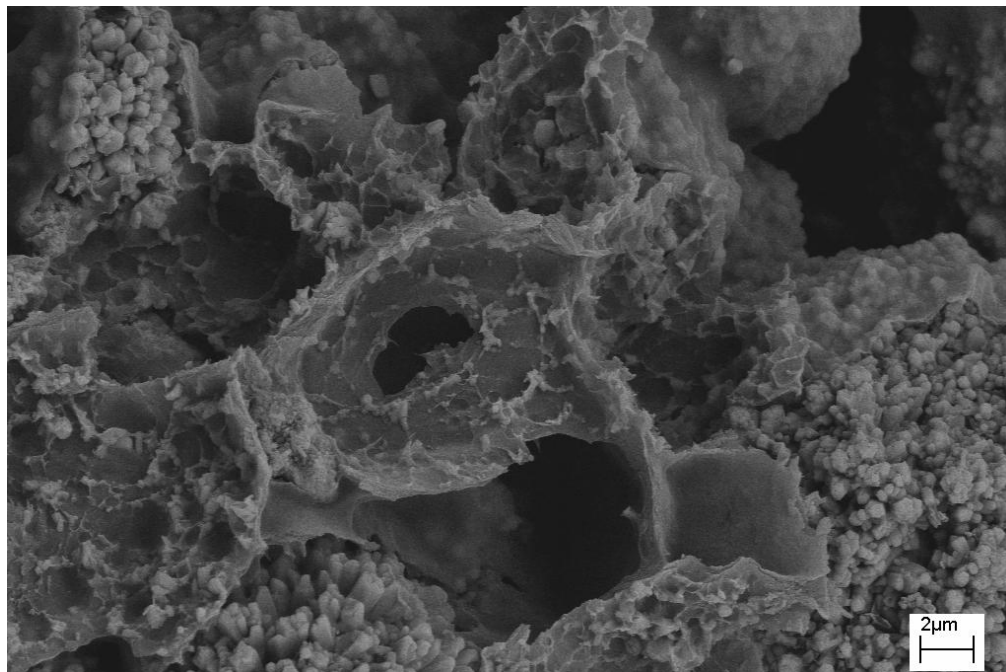
Figure 3.9: SEM of HACSMA15 fracture surface shows a close up view of hydroxyapatite particle pull out location.

The case is also the same for the composites which uses acetic acid. Figure 3.10 shows the fracture surface of the HACSAC15 made with acetic acid. The result is even more pronounced compared to HACSMA15 showing plenty of particles pull out adhesive failure.
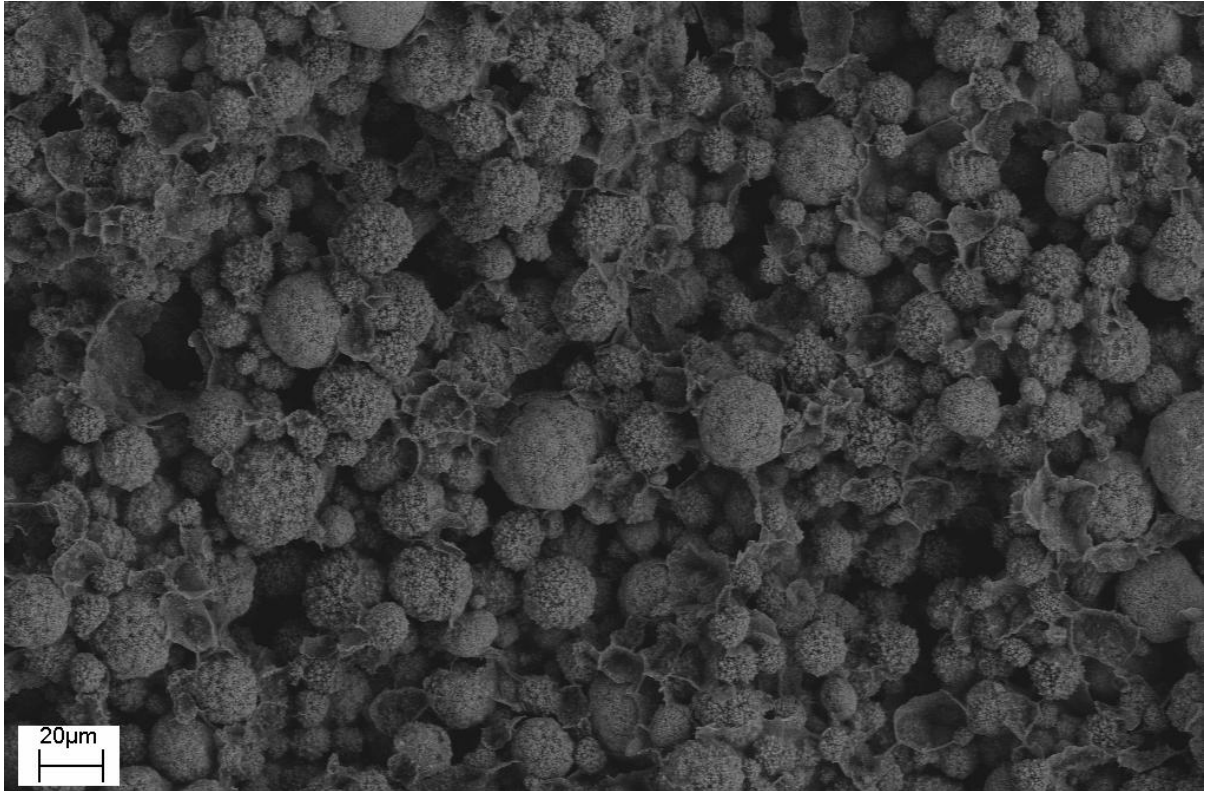
Figure 3.10: SEM of HACSAC15 fracture surface. Particle pull out locations appear throughout.

The consistency of the presence of adhesive failure throughout the composites immersed with sodium hydroxide but their absence in the composite that was not immersed in sodium hydroxide means that sodium hydroxide is the main cause. The immersion in sodium hydroxide weakened the bonding between chitosan and hydroxyapatite. This weakening effect is shown by the decrease of flexural strength and elastic modulus of HACSMA20 after immersion in sodium hydroxide to 1/3 the initial values as discussed above.

25

Chapter 4 **Chemical Characterization**

Understanding the chemical interaction between the different components of the composite is very important tool that can help greatly in the attempts to enhance the composite's properties. The chemical interactions between the different components of the composite were investigated using Fourier transform infrared spectroscopy (FTIR), and X-Ray Absorption Fine Structure (XAFS).

4.1 FTIR

FTIR obtains the infrared absorption spectrum by shining a light beam with different frequencies at a sample and measuring how much of that beam is absorbed. A fast Fourier transform is used to determine which frequencies of light were absorbed. Different set of frequencies are shined at a time.

The absorption spectrum of a sample depends on the bond structures within it; the arrangement, and strength of chemical bonds as well as the sample thickness.

4.1.1. Sample Preparation

In order to characterize the composite's chemical interactions, two specimens were used for FTIR analysis. It was desired that the samples be thin films, because thick samples exhibited very high absorption across the spectrum.

Samples for doing the FTIR spectroscopy were made by the following procedures. First, 0.101g of malic acid was dissolved in 12.5g of water. Once all the malic acid has been dissolved, 0.134g of chitosan was added into the malic acid solution. This solution was vigorously stirred until the chitosan seemed homogenously dissolved. A droplet of this solution was dropped on a slide. The slide was left on room temperature to dry overnight. The result after drying is a thin film of chitosan dissolved in malic acid solution.

Another sample was made by adding 0.015g of hydroxyapatite to the chitosan and malic acid solution. After vigorous stirring of the Hydroxyapatite until homogenous distribution is reached, a droplet of the resulting Hydroxyapatite/chitosan/malic acid solution was dropped on a slide. The slide was left on room temperature to dry overnight. The result after drying is a thin film of hydroxyapatite/chitosan dissolved in malic acid solution with very low concentration of hydroxyapatite.

4.1.2. Characterization

The chemical interaction between the components of the composite will be investigated by Fourier transform infrared spectroscopy (FTIR). FTIR spectroscopy was done using Thermo Nicolet Magna 860 & Continuum IR Microscope at the National Synchrotron Light Source in Brook Haven National lab (NY, USA) at the U2B beam line. The scans were done with 128 scans, a spectral resolution of 4 cm^{-1}, an aperture size of 15 μm x 15 μm, and a MCT detector. The FTIR spectroscopy was done for the chitosan in malic acid sample with no Hydroxyapatite, and also for the chitosan in malic acid with Hydroxyapatite sample. For the latter, the spectroscopy was done starting from a location further away from a

27

Hydroxyapatite particle and repeating the spectroscopy as the location was moved closer to

the Hydroxyapatite particle until the particle was reached as shown below (Figure 4.1)
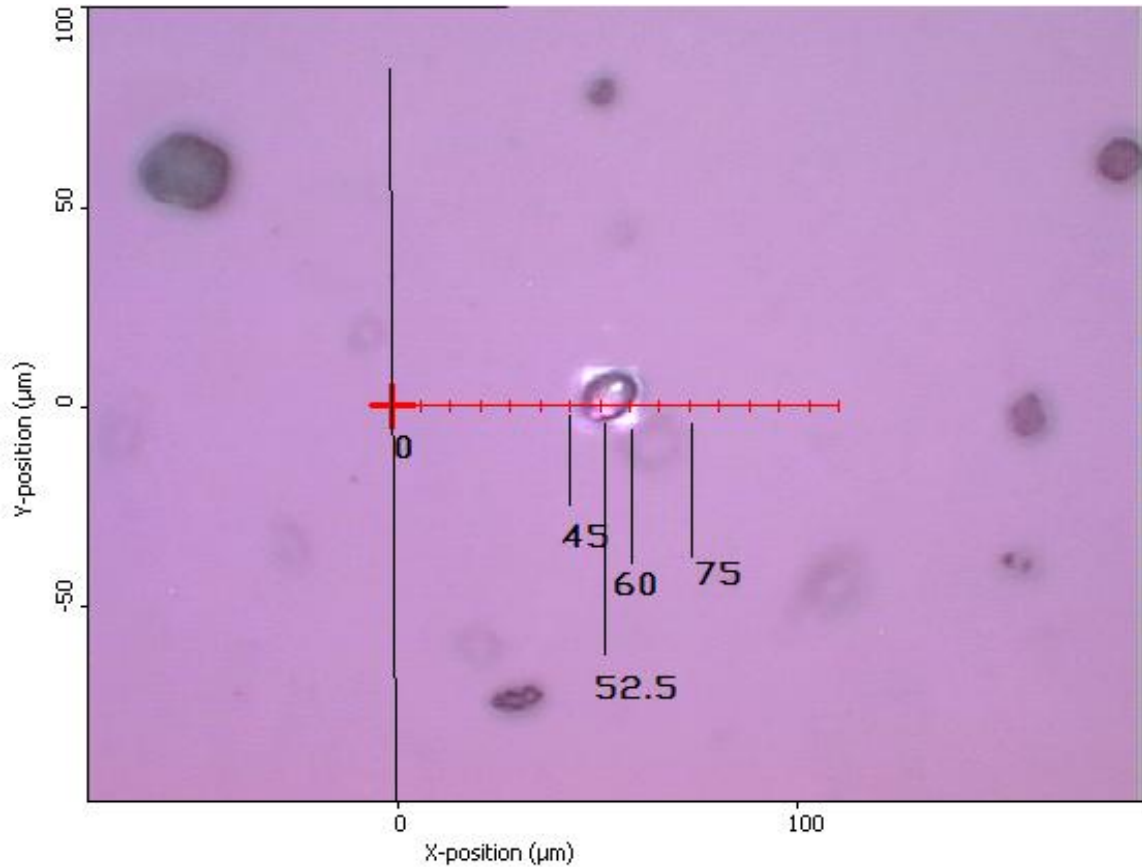
Figure 4.1: The location in the hydroxyapatite/chitosan/malic acid sample where FTIR was done. The FTIR was started at the location shown by the + mark at 0. The FTIR was repeated as the location was moved a step to the right. Each step is 7.5 µm. The particle between positions 45 and 60 is Hydroxyapatite particle.
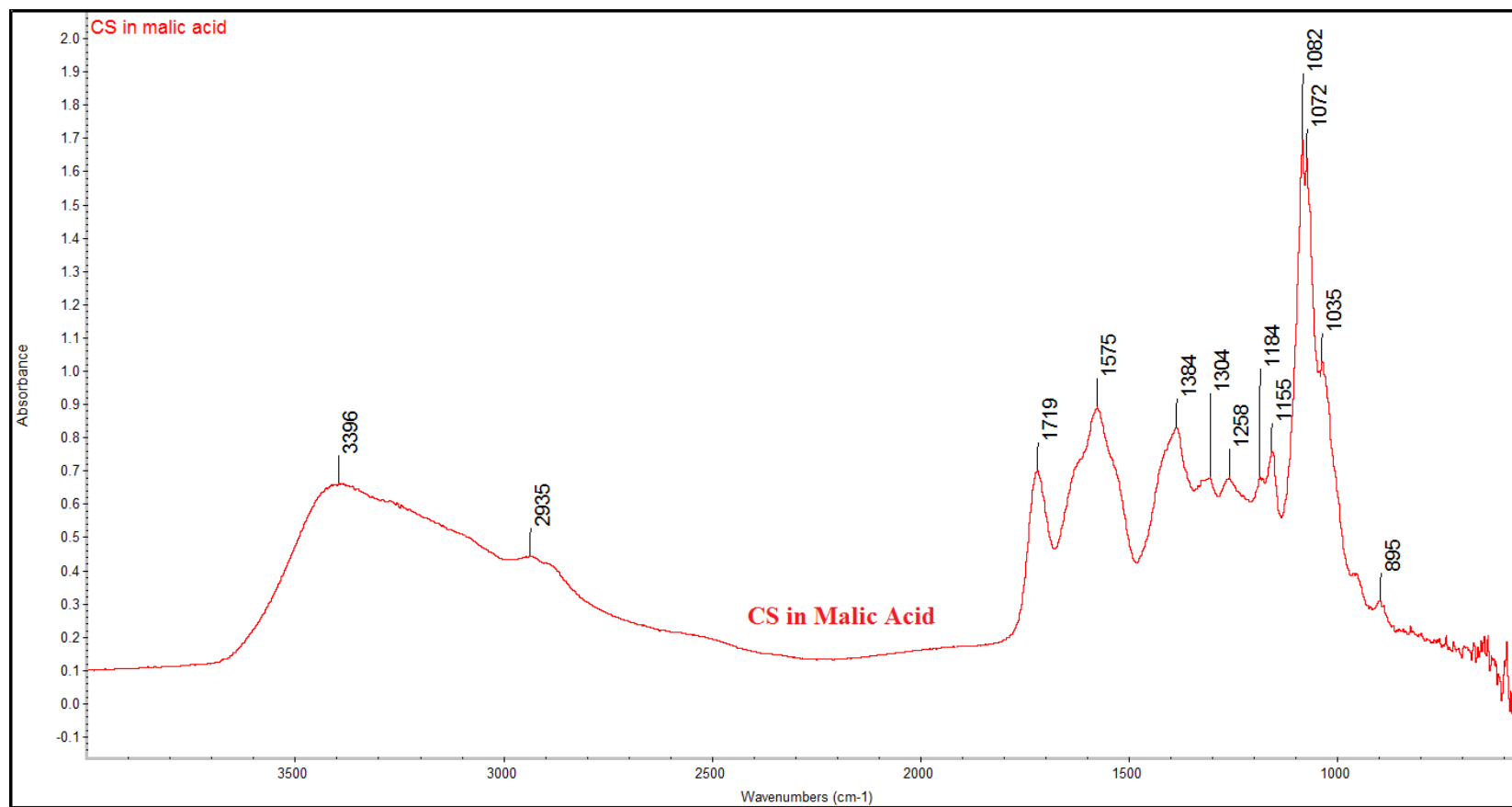
Figure 4.2: FTIR spectra of chitosan dissolved in malic acid
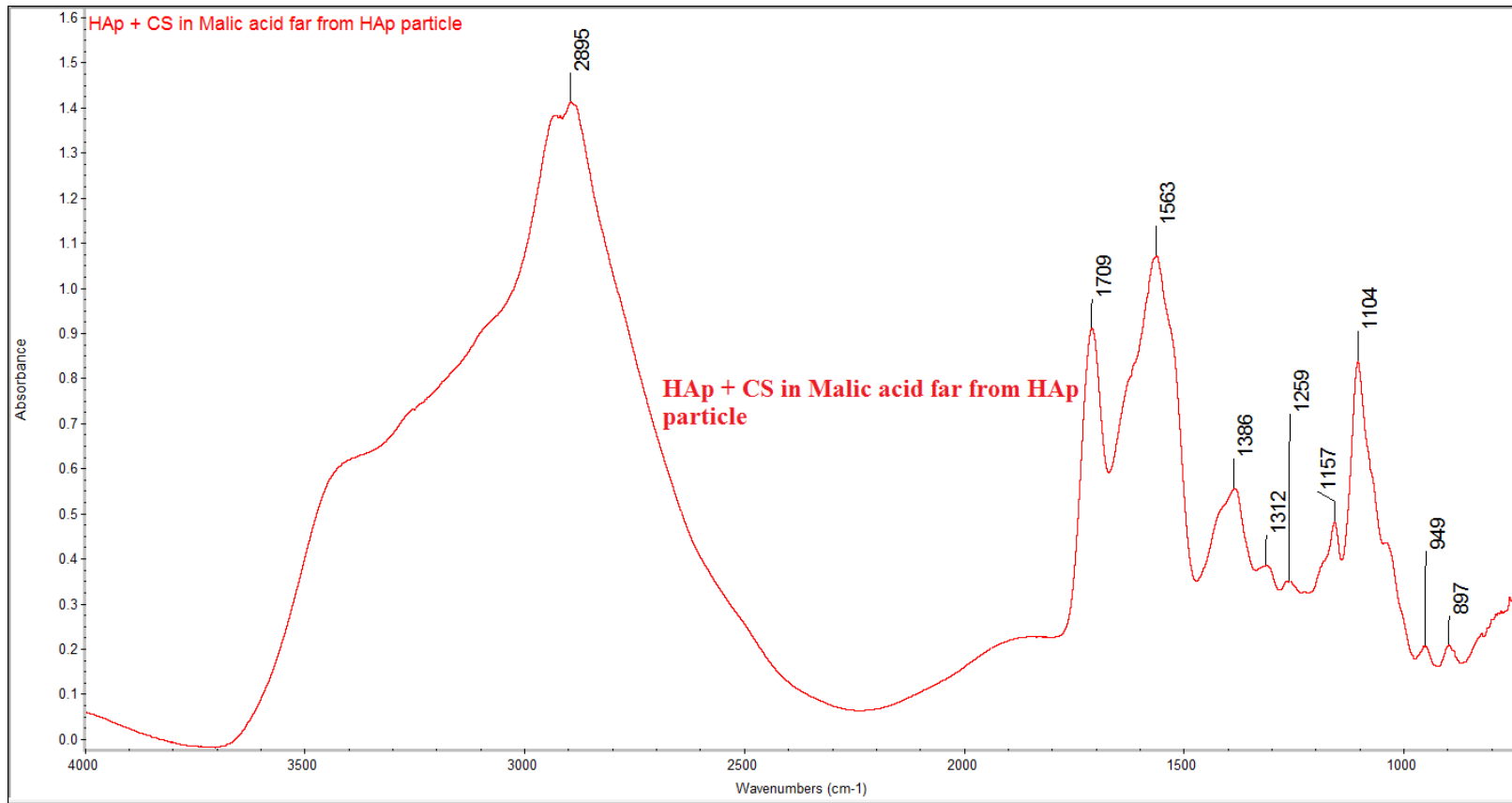
Figure 4.3: FTIR spectra of Hydroxyapatite/chitosan dissolved in malic acid far from a Hydroxyapatite particle (position 0 μm in Figure 4.1)

30
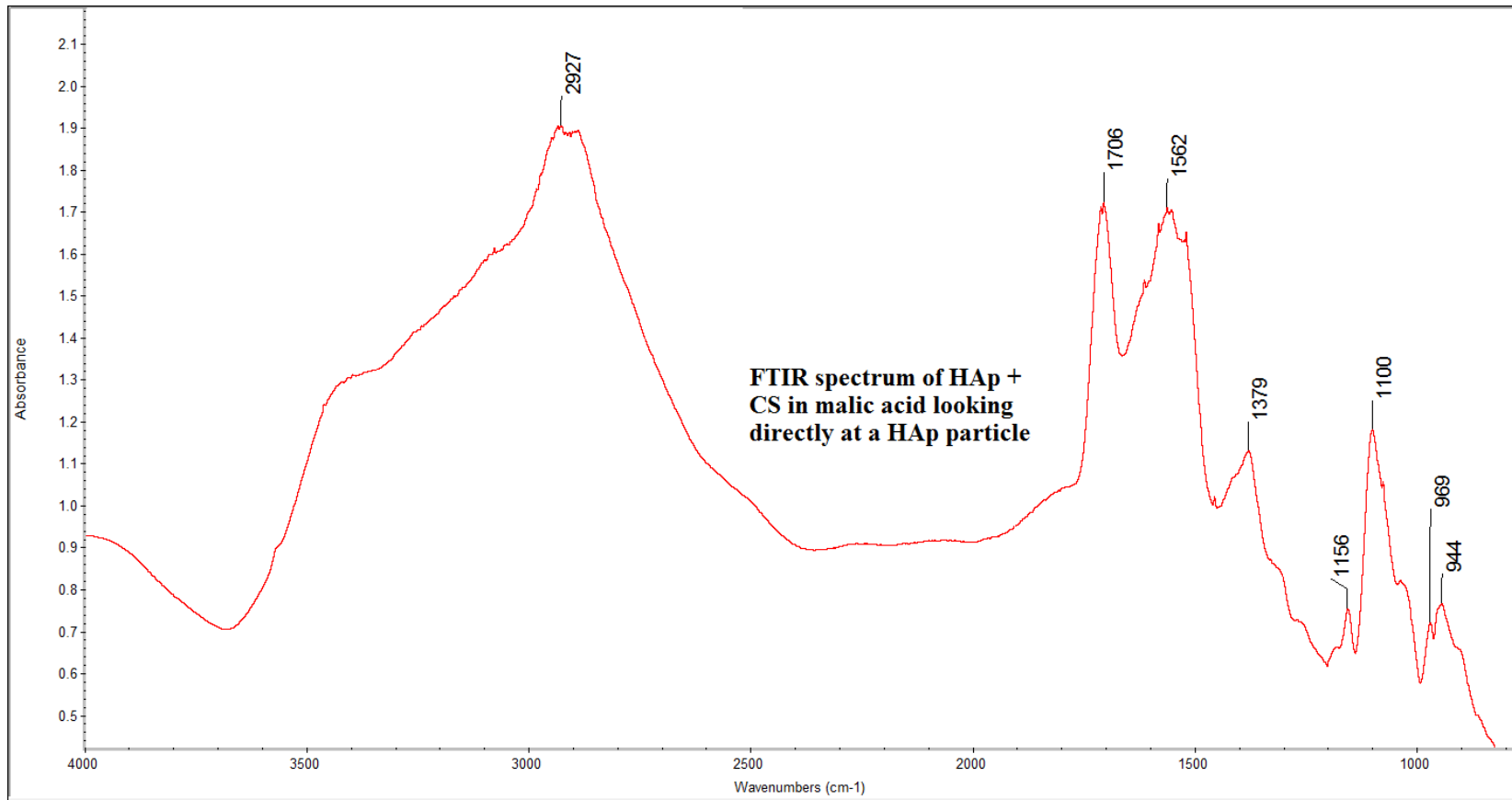
Figure 4.4: FTIR spectra of Hydroxyapatite/chitosan composite dissolved in malic acid directly on top of a Hydroxyapatite particle (position 52.5µm in Figure 4.1)
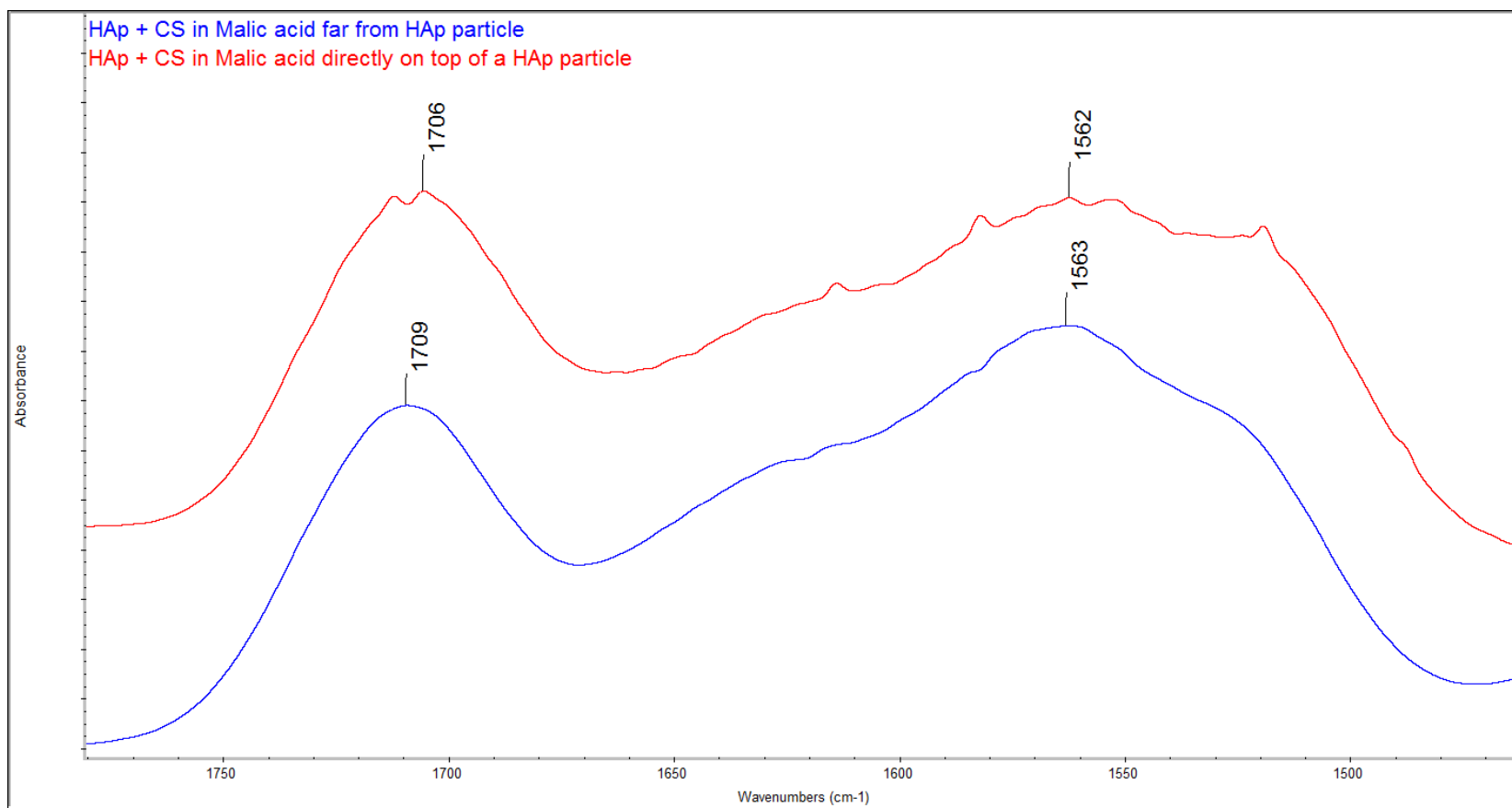
Figure 4.5: A close up view (1470-1780 cm^{-1}) of the FTIR spectra of Hydroxyapatite/chitosan dissolved in malic acid comparing the spectra of that taken directly on top of a Hydroxyapatite particle (position 52.5μm in Figure 4.1) and that taken further away from the Hydroxyapatite particle (i.e. position 52.5μm in Figure 4.1)

32

4.1.3.1. Chitosan and Malic Acid Chemical Interactions

FTIR data revealed very important information about the interaction between the malic acid, chitosan, and Hydroxyapatite. The FTIR spectroscopy of the chitosan dissolved in the malic acid solution is shown in Figure 4.2 above. Some peaks which are characteristic of chitosan such as the amide I absorbance band at 1660 that is associated with the C=O in the acetylated unit of the chitosan [28] has disappeared. This is an indication that the malic acid reacts with the amino group of the N-acetyl-D-glucosamine units. Another characteristic peak of chitosan is the –NH2 peak at 1590[29]. This peak has been shifted to 1575 which indicates that the malic acid reacted with amino group in the deacetylated units too. Other important characteristic peaks that can be observed with no change are the bridge C-O-C stretch at 1155 and the skeletal C-O stretch at 1081 and 1035 [30]. This indicates that the malic acid did not interact with that bridge in between the units making the chitosan. The peak at 3396 relates to the -OH stretch vibration in the hydroxyl.

4.1.3.2. Hydroxyapatite/chitosan/Malic acid chemical interactions

The chemical interactions between Hydroxyapatite, chitosan, and malic acid were investigated by examining the FTIR spectroscopy of the sample with the Hydroxyapatite dispersed in the chitosan and malic acid matrix (Figure 4.3 - 4.5). It was noted that the FTIR spectroscopy at locations further from the Hydroxyapatite particle exhibited similar characteristics regardless of the distance from the Hydroxyapatite particle. Figure 4.3 shows

a typical FTIR spectrum away from the Hydroxyapatite particle. The FTIR spectroscopy only changed when looking directly at a Hydroxyapatite particle in the chitosan/malic acid matrix (Figure 4.4 and Figure 4.5).

As can be seen in Figure 4.3, the FTIR spectroscopy of the Hydroxyapatite and chitosan in malic acid further away from the Hydroxyapatite particle is slightly different from that of chitosan in malic acid only. The 1718 C=O peak for the chitosan in malic acid was shifted to 1709. Similarly, the 1575 –NH2 peak was shifted to 1563. Additionally, the 1082 skeletal C-O stretch was shifted to 1104. The fact that all those changes occurred far from the Hydroxyapatite particle suggests that something has come off the Hydroxyapatite particle and has interacted with the chitosan and malic acid throughout the matrix. The change in the amino group of the chitosan indicates that Hydroxyapatite is reacting with the chitosan in that functional group. However, since the malic acid also reacted with the amino groups as concluded in 3.1, the C=O bond in the malic acid was affected too. One thing that is not clear is why the 1082 C-O skeletal stretched shifted to 1104.

When looking directly at the Hydroxyapatite particle in the middle of the chitosan and malic acid matrix, the resulting FTIR spectroscopy can be seen in Figure 4.4 and Figure 4.5 above. This spectrum is different from the one far from the Hydroxyapatite particle in that there are new small peaks between 1500 and 1600. Also, there is a new peak at 969. The small peaks from 1500 to 1600 superimposed on the bigger 1562 peak suggests the presence of carboxyl. The fact that these peaks appeared only when looking directly at the Hydroxyapatite particle suggests that Hydroxyapatite is interacting with the carboxyl in the malic acid. The carboxyl might be the glue that attaches the Hydroxyapatite particle to the chitosan matrix. The new peak found at 969 might be related to the v_1 P-O symmetric stretch [31].

34

4.1.4. FTIR Results summary

The FTIR spectroscopy analysis shows that the amino group both in the acetylated and deacetylated units in chitosan and the carboxyl in malic acid are the chemical glue that holds chitosan-Hydroxyapatite composite together.

4.2. XAFS

X-Ray Absorption Fine Structure (XAFS) is a technique that measures the X-ray absorption coefficient, μ. The absorption of a material depends on the type of the atoms in the sample, and the thickness of the sample. The absorption coefficient is given by the equation below.

$$\mu(E) = \frac{-1}{d} \ln\left(\frac{I_t}{I_0}\right)$$

Where d is the thickness of the material, I_t is the number of X-ray photons that are transmitted through the sample, and I_0 is the number of X-ray photons shone on the sample. The absorption coefficient increases dramatically as the energy of the shined light equals that of the binding energy of an electron in an atom in the sample. As the x-ray photon hits an electron with energy more than the binding energy, the energy of the photon is transferred to the ejected photoelectron which can be scattered by the neighboring atoms. The scattering of the photoelectron wave causes interference between the outgoing and the backscattered electron wave. XAFS is brought about due to these interferences.

35

For each atom, there exist a different set of absorption edges relating to different binding energies of the atom's electrons. This can be advantageous when it is desired to look at a specific element, by limiting the energy range at which to take the spectrum to that near the desired absorption edge of that element.

The XAFS is being study in order to better understand the role of the hydroxyapatite's phosphate in the composite's chemical interaction. The FTIR results indicate that something comes off the hydroxyapatite particle and gets distributed throughout the matrix as well as chemically interact with the chitosan-malate matrix. Additionally, it was found that there were some interactions between hydroxyapatite and chitosan-malate solution. The XAFS data would give us a better understanding about this aspect.

4.2.1. Sample preparation

The samples were prepared as explained in section 2.1 except for the soaking in NaOH. A small piece of the composite was taken and broken down into smaller flakes. Three different composites were prepared in addition to the pure hydroxyapatite and nano-hydroxyapatite. Composites with Hydroxyapatite/chitosan ratio of about 15 and 12 were used. The malic acid powder/chitosan powder ratio was 0.75 for both and molarity was 0.25M as before. Another sample was made with hydroxyapatite/chitosan and malic acid powder/chitosan powder ratios of 12 and 1 respectively. The same amount of water content was used when dissolving the chitosan yielding a sample with a higher malic acid concentration.

36

4.2.3. XAFS Characterization

The samples were characterized by XAFS at the National Synchrotron Light Source (NSLS) at Brookhaven National Laboratory (Upton, NY) using beam line X15B with energy level ranging from 2100 eV to 2750 eV. The result was processed using Athena software package.

4.2.3. XAFS Results

The results of the XANES part of the XAFS data is shown below in Figure 4.6. As can be observed from the graphs, there is no shifts in the near edge energy range for any of the different samples. The location of the hydroxyapatite peak shows no shifts in any of the different samples. This indicates that most of the phosphate is still enclosed inside the hydroxyapatite particle.
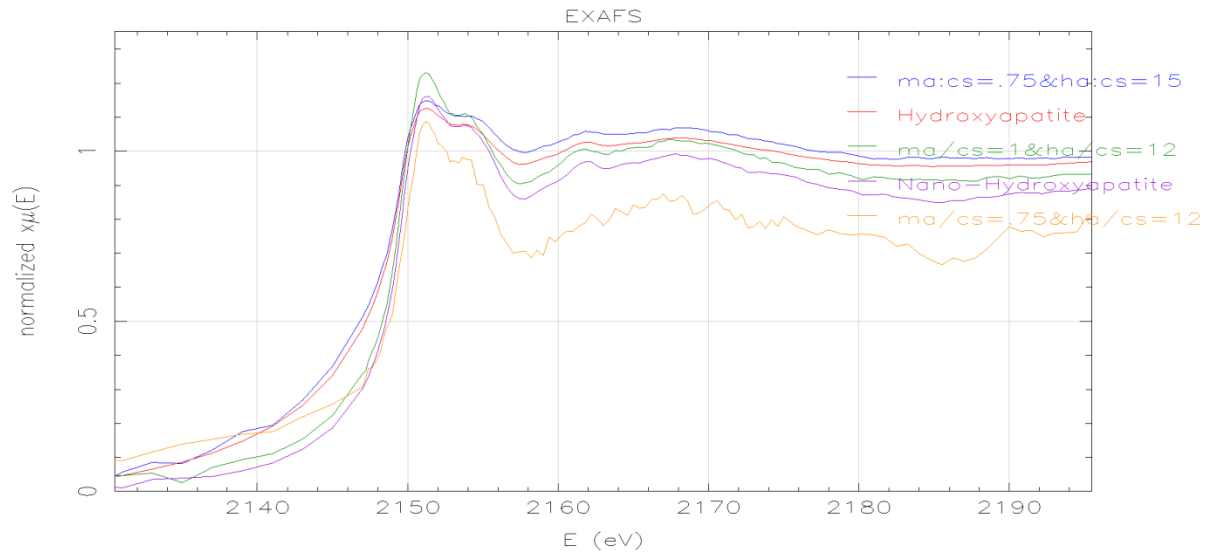
EXAFS

Figure 4.6: The XANES part of the XAFS data for all samples is shown above. The data were normalized with respect to the pre-edge line and post-edge line. ma:cs is the malic acid powder to chitosan powder ratio. ha:cs is the hydroxyapatite to chitosan powder ratio

Looking closely at the spectra of the sample with MA:CS=0.75 and HA:CS=15 and the pure hydroxyapatite sample Figure 4.7, it can be noticed how well the composite follows the structure of the pure hydroxyapatite. In the other hand, the sample with MA:CS=1 and HA:CS=12 show more resemblance to the nano-hydroxyapatite structure Figure 4.8. A comparison of the pure hydroxyapatite and non-hydroxyapatite is shown in Figure 4.9 below. The difference between the sample resembling the nano-hydroxyapatite and the one resembling the micro-hydroxyapatite is both their malic acid to chitosan ratio and chitosan to hydroxyapatite ratio. However, it cannot be told which is causing the change due to the fact that the fifth data sample is noisy and cannot used for comparison and to help in pinpointing the cause.

38

One hypothesis that might explain this is that the changing composition makes the hydroxyapatite act more like nano-hydroxyapatite by the dissolution of some of the phosphate during the production of the composite.

It was determined from the FTIR study that the carboxyl is bonding to the hydroxyapatite surface. Additionally, it was determined that some part of the hydroxyapatite has been dispersed throughout the matrix. The results from the XAFS suggest that the hydroxyapatite here is acting like nano-hydroxyapatite. This might be due to the fact that the changing composition of the composite causes dissolution of some of the phosphates which are now more exposed to the X-ray beam since they are being trapped inside the 10-20 micron hydroxyapatite particle. This exposure of the phosphate makes it more like a nano hydroxyapatite in that there is more phosphate per surface area in the nano hydroxyapatite that is exposed to the X-ray beam. It can be concluded that this is caused by the increase in malic acid content due to the fact that it is the malic acid that is reacting chemically with the hydroxyapatite as the FTIR results suggest.
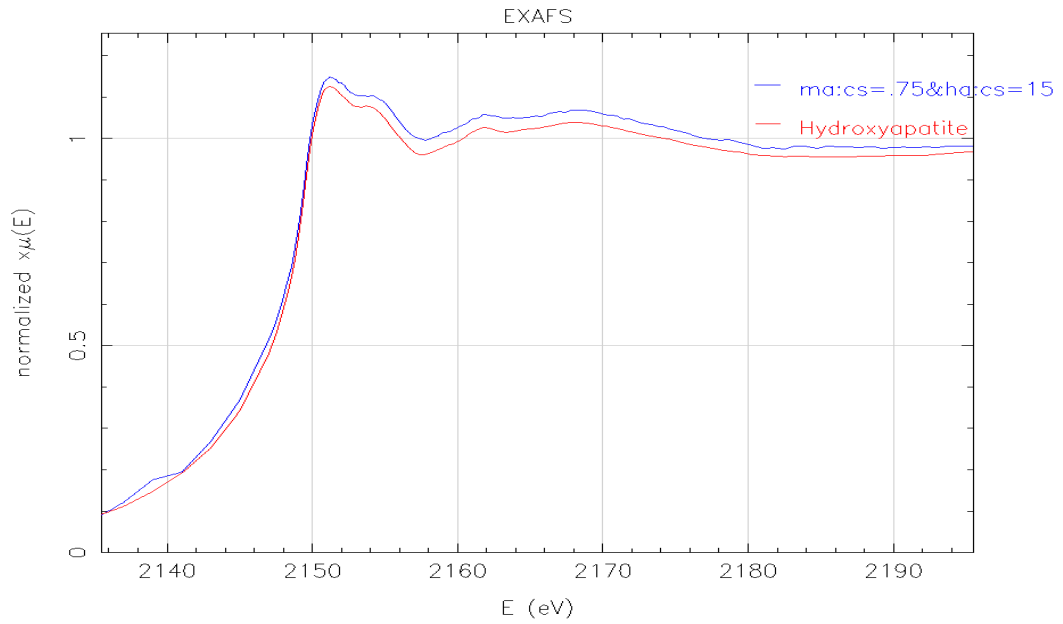
Figure 4.7: The XANES part of the XAFS data comparing pure hydroxyapatite and a composite with MA:CS ratio of 0.75 and HA:CS ratio of 15
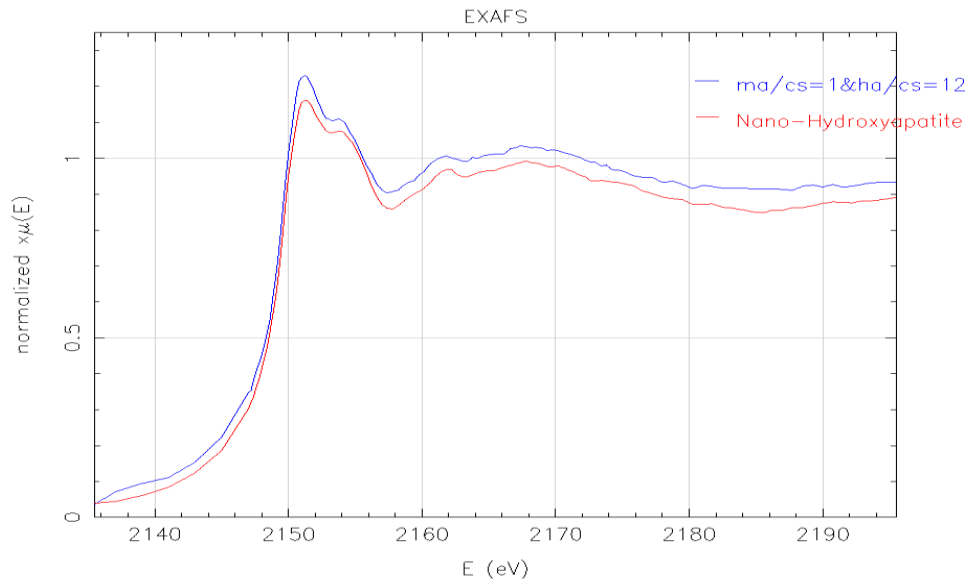

Figure 4.8: The XANES part of the XAFS data comparing pure hydroxyapatite and a composite with MA:CS ratio of 1 and HA:CS ratio of 12
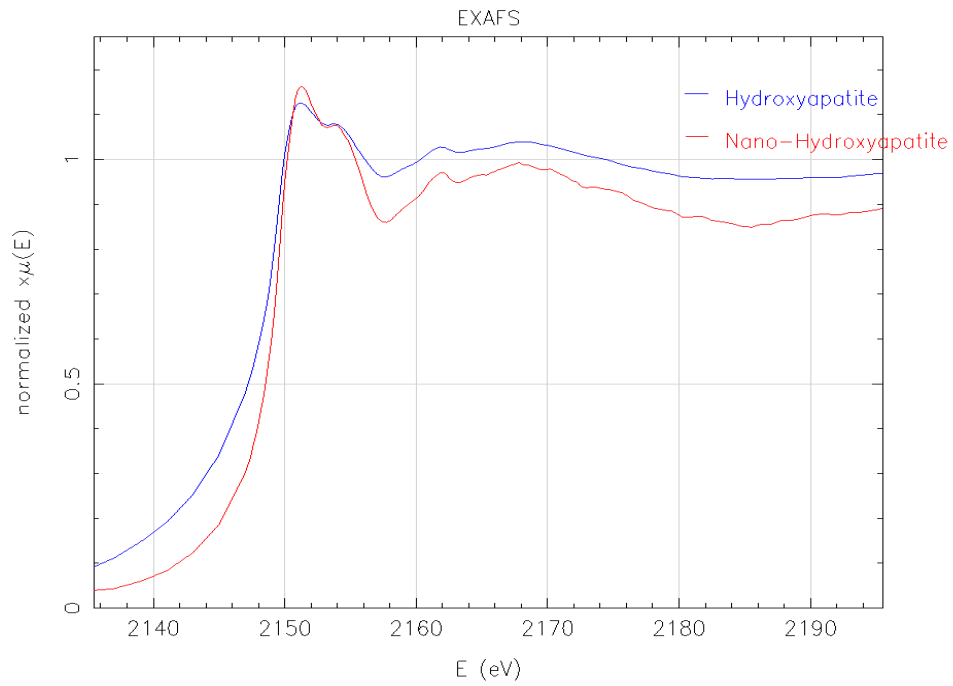
Figure 4.9: The XANES part of the XAFS data comparing pure hydroxyapatite and nano-hydroxyapatite

Chapter 5 **Conclusion**

In this study, hydroxyapatite/chitosan composite has been studied and characterized mechanically and chemically for varying processing conditions. The processing conditions that were studied include immersion in sodium hydroxide, inclusion of nano and micro hydroxyapatite particles, as well as changing concentration of chitosan in the composite.

It was found that immersion in sodium hydroxide has very detrimental effect on the composite cohesion. The sodium hydroxide weakened the interaction between the hydroxyapatite particle and the chitosan matrix. This weakening was so significant that it reduced the flexural strength and elasticity of the composite by a factor of 1/3. It was also determined that mechanical properties of the wet samples were very weak; a 100 times weaker than its dry counterpart which has been soaked in sodium hydroxide.

Some correlation between mechanical properties and other processing parameters were found such as the increase in strength when adding more hydroxyapatite. Additionally, it was determined that acetic acid usage results in similar properties as composites using malic acid. This was explained by the existence of the carboxyls in both acetic and malic acids. It was hypothesized that the malic acid and chitosan react very similarly to chitosan and hydroxyapatite due to them both having the carboxyl group which was found by FTIR to be the main glue that holds the composite together in the case of malic acid.

The nano and micro hydroxyapatite mixture /chitosan composite showed slight decrease in strength as opposed to the micro-hydroxyapatite/chitosan composite. One possible explanation for the decrease in strength can be attributed to having a lot more hydroxyapatite surface area due to the inclusion of nano particles than there was with the micro composite

with the same mass ratio. It was hypothesized, that the composite was over saturated with hydroxyapatite surface.

With no sodium hydroxide, the chemical interactions between the composite's components were characterized. It was found by FTIR that there was some good chemical interaction between all components of the composite. It was concluded that the amino group both in the acetylated and deacetylated units in chitosan and the carboxyl in malic acid are the chemical glue that holds chitosan-Hydroxyapatite composite together.

Chapter 6 **Future Work**

Some recommendations for future work include:

- Finding a better way to improve the washout resistance of the composite

  - One idea I was going to try was adding the sodium hydroxide in the initial processing of the sample to balance the PH level when the composite is in the paste phase.

- Testing the mechanical composite for various concentrations of chitosan and inclusion of various fractions of nano-particles without immersion in sodium hydroxide to get a better idea about the effect of these parameters.

- Trying different kind of acids that do not have carboxyls

  - See the effect on the mechanical strength

  - See the effect on the chemical interactions

- Washing the hydroxyapatite powder in deionized water before using it to make the composite to wash out any residual phosphate on the surface of the particles, and study the effect of that on the mechanical and chemical properties of the composite

- Doing cell culturing studies as a function of the various processing parameter

Chapter 7 **References**

1] Xuan Cai et al., "Preparation and characterization of homogeneous chitosan–polylactic acid/hydroxyapatite nanocomposite for bone tissue engineering and evaluation of its mechanical properties," *Acta Biomaterialia*, vol. 5, pp. 2693-2703, 2009.

2] Guoping Chen, Takashi Ushida, and Tetsuya Tateishi, "Scaffold Design for Tissue Engineering," *Macromolecular Bioscience*, vol. 2, no. 2, pp. 67-77, 2002.

3] Lijun Kong et al., "Preparation and characterization of nano-hydroxyapatite/chitosan composite scaffolds," *Journal of Biomedical Materials Research. Part A*, vol. 75, no. 2, pp. 275-282, 2005.

4] Haiguang Zhao, Lie Ma, Changyou Gao, and Jiacong Shen, "Fabrication and properties of mineralized collagen-chitosan/hydroxyapatite scaffolds," *Polymers for Advanced Technologies*, vol. 19, pp. 1590-1596, 2008.

5] Isamu Yamaguchi and et al., "The effect of citric acid addition on chitosan/hydroxyapatite composites," *Colloids and Surfaces*, vol. 214, pp. 111-118, 2003.

6] Rachel Auzely and Marguerite Rinaudo, "Controlled Chemical Modifications of Chitosan. Characterization and Investigation of Original Properties," *Macromolecular Bioscience*, vol. 3, pp. 562-565, 2003.

7] C. A. Custodio, C. M. Alves, R. L. Reis, and J. F. Mano, "Immobilization of fibronectin in chitosan substrates improves cell adhesion and proliferation," *Journal of Tissue Engineering and Regenerative Medicine*, vol. 4, pp. 316-323, 2010.

8] Eugene Khor, "Implantable Applications of Chitin and Chitosan," *Biomaterials*, pp. 2339-2347, 2003.

9] Dunia Mercedes Garcııa Cruz et al., "Chitosan microparticles as injectable scaffolds for tissue engineering," *Journal of Tissue Engineering and Regenerative Medicine*, vol. 2, pp. 378-380, 2008.

10] Sundararajan V. Madihally and Howard W.T. Matthew, "Porous chitosan sca!olds for tissue engineering," *Biomaterials*, vol. 20, pp. 1133-1142, 1999.

11] Elena F. Burguera, Hockin H. K. Xu, and Michael D. Weir, "Injectable and Rapid-Setting Calcium Phosphate Bone Cement with Dicalcium Phosphate Dihydrate," *Journal of Biomedical Materials Research Part B: Applied Biomaterials*, vol. 77B, no. 1, pp. 126-134, 2005.

12] Limin Sun, Hockin H. K. Xu, Shozo Takagi, and Laurence C. Chow, "Fast Setting Calcium Phosphate Cement–Chitosan Composite: Mechanical Properties and Dissolution Rates," *Journal of Biomaterials Applications*, vol. 21, pp. 299-315, 2007.

13] Hockin H. K. Xu, Shozo Takagi, and Laurence C. Chow Janet B. Quinn, "Fast-setting calcium phosphate scaffolds with tailored macropore formation rates for bone regeneration," *Journal of Biomedical Materials Research Part A*, vol. 68A, no. 4, pp. 725-734, 2003.

14] Vitor Correlo, Elisabete Pinho, Iva Pashkuleva, and Mrina Bhattacharya, "Water Absorption and Degradation Characteristics of Chitosan-Based Polyesters and Hydroxyapatite Composites," *Macromolecular Bioscience*, vol. 7, pp. 354-363, 2007.

15] Junjie Li et al., "Surface characterization and biocompatibility of micro- and nano-hydroxyapatite/chitosan-gelatin network films," *Materials Science and Engineering C*, vol. 29, pp. 1207-1215, 2009.

16] Zhang Li, Li Yubao, Zuo Yi, Wu Lan, and John A. Jansen, "In vitro and in vivo evaluation on the bioactivity of ZnO containing nano-hydroxyapatite/chitosan cement," *Journal of Biomedical Materials Research Part A*, vol. 93, pp. 269-279, 2010.

17] Prapaporn Jongwattanapisan et al., "In vitro study of the SBF and osteoblast-like cells on hydroxyapatite/chitosan–silica nanocomposite," *Materials Science and Engineering C*, vol. 31, pp. 290-299, 2011.

18] Hassna R. Ramay, Zhensheng Li, Enoch Shum, and Miqin Zhang, "Chitosan-Alignate Porous Scaffolds Reinforced by Hydroxyapatite Nano- and Micro-Particles: Structual, Mechanical, and Biological Properties," *Journal of Biomedical Nanotechnology*, vol. 1, pp. 151-160, 2005.

19] Lijun Kong et al., "A study on the bioactivity of chitosan/nano-hydroxyapatite composite scaffolds for bone tissue engineering," *European Polymer Journal*, vol. 42, pp. 3171-3179, 2006.

20] Haruhiko Kashiwazaki et al., "Fabrication of Porous Chitosan/Hydroxyapatite Nanocomposites: Their Mechanical and Biological Properties," *Bio-Medical Materials and Engineering*, vol. 19, pp. 133-140, 2009.

21] Zhang Li et al., "Preparation and in vitro investigation of chitosan/nano-hydroxyapatite composite used as bone substitute materials," *Journal of Materials Science: Materials in Medicine*, vol. 16, pp. 213-219, 2005.

22] W.W. Thein-Han and R.D.K. Misra, "Biomimetic chitosan–nanohydroxyapatite composite scaffolds for bone tissue engineering," *Acta Biomaterialia*, vol. 5, pp. 1182-1197, 2009.

23] Sung Eun Kim et al., "Designing a highly bioactive 3D bone-regenerative scaffold by surface immobilization of nano-hydroxyapatite," *Journal of Materials Chemistry*, vol. 18, pp. 4994-5001, 2008.

24] Seong-Hoon Kim et al., "Preparation of High Flexible Composite Film of Hydroxyapatite and Chitosan," *Polymer Bulletin*, vol. 62, pp. 111-118, 2009.

25] K. Madhumathi et al., "Wet chemical synthesis of chitosan hydrogel–hydroxyapatite composite membranes for tissue engineering applications," *International Journal of Biological*

46

Macromolecules, vol. 45, pp. 12-15, 2009.

[26] Atsushi Matsuda, Toshiyuki Ikoma, Hisatoshi Kobayashi , and Junzo Tanaka, "Preparation and mechanical property of core-shell type chitosan/calcium phosphate composite fiber," *Materials Science and Engineering C*, vol. 24, pp. 723-728.

[27] Karl Nelson, *Processing and Characterization of Chitosan and Hydroxyapatite filled Polymer Composites. Masters Thesis*. Stony Brook, NY: Stony Brook University, 2009.

[28] A. Pawlak and M. Mucha, "Thermogravimetric and FTIR studies of chitosan blends," *Thermochimica acta*, pp. 153-166, 2002.

[29] E. Piron and A. Domard, "Interaction between chitosan and uranyl ions. Part 2. Mechanism of interaction," *International Journal of Biological Macromolecules*, pp. 33-40, 1998.

[30] Bing Geng and et al, "Preparation of chitosan-stabilized Fe nanoparticles for removal of hexavalent chromium in water," *Science of the Total Environment*, pp. 4994-5000, 2009.

[31] A. Stoch and et al., "FTIR study of electrochemically deposited hydroxyapatite coatings on carbon materials," *Journal of Molecular Structure*, pp. 389-396, 2002.